Dear Dr. Frank Dentener,

Please find below our itemized responses to the referees' comments. We have addressed all the comments, and incorporated the comments/suggestions in the revised manuscript.

Thank you very much for your consideration.

Sincerely,

Xiuying Zhang

On behalf of all co-authors

Response to Referee #1

Received and published: 3 May 2019

This manuscript estimated global surface NH_3 concentration based on satellite retrievals and the temporal variation of NH_3 concentration was also presented. The study was well designed and the results are also important for evaluate NH_3 pollution in the world. The major comments to the manuscript are as follows.

The authors appreciate the valuable suggestions given by Referee #1 for improving the overall quality of the manuscript. In this document, we describe how we addressed the reviewer's comments. Detailed responses to each comment are given below (in blue).

1 Lines 278-280, for comparing the satellite-derived and measured surface NH_3 concentrations, are there any criterions to choose the sites which measured surface NH_3 concentrations? This is because satellite-derived surface NH_3 concentration in a grid (0.25^o latitude × 0.25^o longitude) is a reflection of the averaged NH_3 concentration in this grid area, but the NH_3 concentration measured at a site may only represent a limited area. For a grid with different sources of NH_3 (e.g., cropland, animal house or feedlot), the NH_3 concentration in this grid may have large spatial heterogeneity, then how to find a site with the surface NH_3 concentration to represent a grid area?

A point-to-grid verification strategy is adopted here, i.e. comparing the measurements at the monitoring stations with the grid values of satellite-derived estimates. We have to admit that this is the uncertainty of our analysis for comparing the satellite-derived and measured surface NH_3 concentrations since the monitoring site may not be representative of a given grid cell for an average retrieved value. We have added the following text to discuss this potential uncertainty in the section of "Validation of satellite-derived surface NH_3 concentrations":

"Notably, we compared the surface NH_3 concentrations at the monitoring stations with

the grid values of satellite-derived estimates directly. This point-to-grid verification strategy may cause uncertainty since the monitoring site location may not be representative of a given grid cell for an average retrieved value.".

2 Lines 282-284, for comparing NH_3 concentrations with different methods, the information on how many measuring sites, and where the sites located should be given for each country or region.

Thanks very much for this good suggestion. We have added the number of measuring sites in each region by the following text:

"IASI-derived surface NH_3 concentrations gained higher consistency with the ground-based measurements in China (R^2=0.71 and RMSE=2.6 μg N m^{-3} for 43 sites) than the US (R^2=0.45 and RMSE=0.76 μg N m^{-3} for 67 sites) and Europe (R^2=0.45 and RMSE=0.86 μg N m^{-3} for 43 sites) at a yearly scale".

The sites locations have been given for each region in Fig. 2 in the manuscript .

3 Lines 284-286, as mentioned in comment 1, the spatial heterogeneity of NH_3 concentration in a grid and the measuring sites location may also cause the differences between satellite-derived and ground-based NH_3 concentration. Thus, this discussion should be added here.

This concern has been addressed in the response to comment 1. Please refer to it.

Besides, the detection limit and precision for deriving NH_3 concentration using the satellite should be given.

Thanks very much for this good suggestion. We have added the following text for clarifications:

"The satellite-derived NH_3 has a detection limit of 0.0025 μg N m^{-3} (2.5 ppb) (Graaf et al., 2018;Van Damme et al., 2014).".

4 Lines 318-320, More details of the location of NH_3 hotspots should be given. In China, where is the eastern China? It seems that there were also NH_3 hotspots in Shannxi, Shanxi, Gansu and Hubei provinces, and there were no hotspot (> 8 ug N m^{-3}) in Xinjiang province in Fig. 4?

Thanks very much for this good comment. We have revised the "eastern China" as

"eastern China (109-122^{o} E, 28-41^{o} N)".

To show more details of the locations of NH_3 hotspots, we have revised the descriptions by the following text:

"We found large areas in eastern China (109-122^{o} E, 28-41^{o} N), Sichuan Basin, Hubei (including Wuhan, Xiangyang and Yichang), Shaanxi (including Xi'an, Baoji, Hanzhong, Weinan), Gansu (Lanzhou and its surrounding areas), Shanxi (including Yuncheng and Changzhi) and northwestern Xinjiang with surface NH_3 concentrations greater than 8 μg N m^{-3} y^{-1}.".

5. Lines 321-324, in fact, more than half the NH_3 emissions in China is caused by animal production. The higher NH_3 concentration in eastern China can also be caused by animal production. More discussion and supporting data should be provided to strengthen the contribution of animal production on NH_3 concentration. This is also true for US and Europe.

Thank you very much for this suggestion. We have carefully checked the NH_3 emissions. In addition to N fertilization, N manure is another major source of NH_3 emissions in China, and the percentage of N manure to NH_3 emissions exceeds 50% (Kang et al., 2016). So we have added the N manure into our analysis in Fig. 4 and Fig. 5 and revised related text in the discussion.

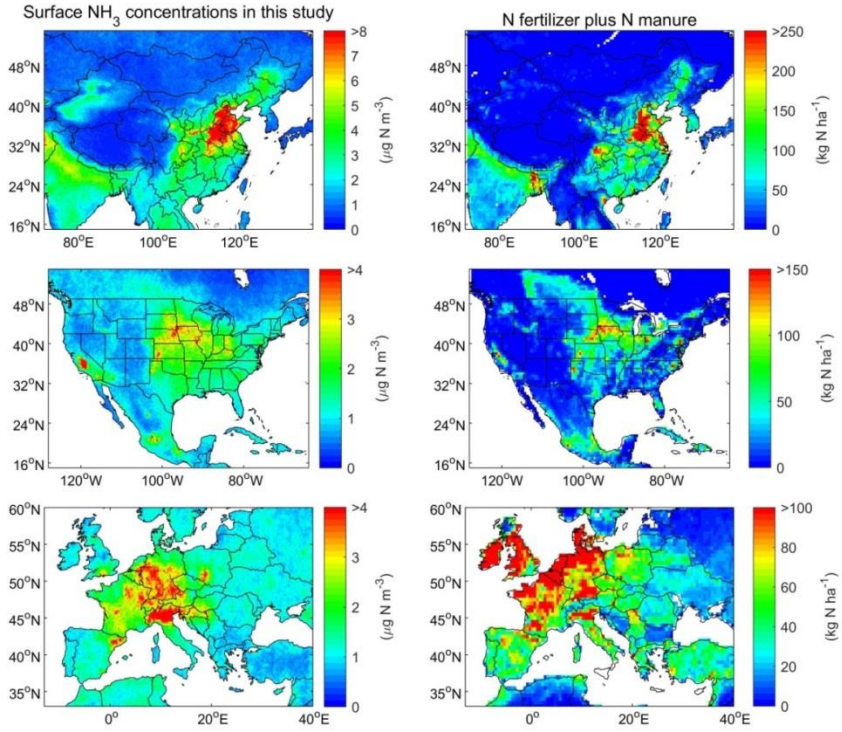

Fig. 4 Spatial distribution of IASI-derived surface NH_3 concentrations, and N fertilizer plus N manure in China, Europe and US.

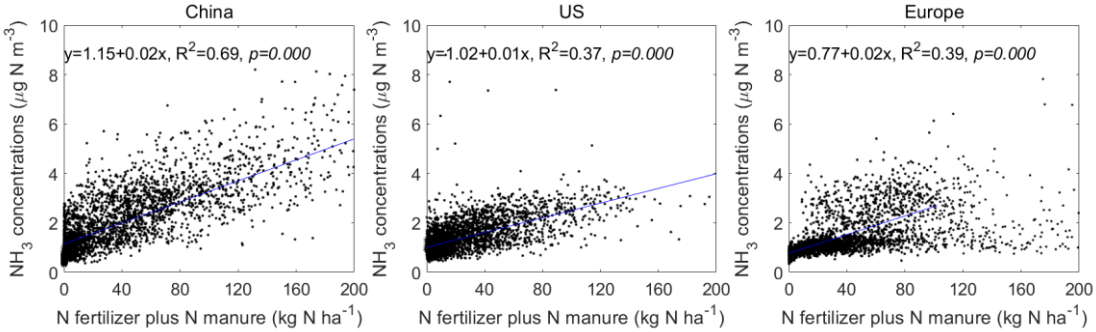

Fig. 5 Comparison of satellite-derived surface NH_3 concentrations, and N fertilizer plus N manure in China, US and Europe. The spatial resolution of satellite-derived surface NH_3 concentrations and N fertilizer plus N manure is 0.25^o and 0.5^o, respectively. We firstly resampled the satellite-derived surface NH_3 concentrations to 0.5^o grids, and then compared it with N fertilizer plus N manure by each grid cell. We obtained the N fertilizer and N manure data produced from McGill University (Potter et al., 2010).

6. Lines 398-402, are there any differences for the seasonal variation of NH_3 concentration in different regions?

Yes. We take a case study on the seasonal NH_3 concentration in two hotspots of eastern China and Guangdong. The maximum surface NH_3 concentration in eastern China occurred in June and July, which coincided with the planting, fertilization

time and higher temperature of the main crops in the region (Van Damme et al., 2015). The maximum surface NH_3 concentration appeared in March in Guangdong, which was also closely related to crop fertilization in these areas (Shen et al., 2009;Van Damme et al., 2014). We have added the following text for clarifications:

"Notably, there is a difference in the seasonal variations of surface NH_3 concentrations between ECH (peaking in June and July) and GD (peaking in March), which was likely related to different crop planting, N fertilization time as well as meteorological factors (Van Damme et al., 2015;Shen et al., 2009;Van Damme et al., 2014).".

7. Lines 486- 488, which sector (crop or animal production) did cause the increase of NH_3 emissions in China in 2008-2015?

We have added the following text to explore the potential reasons:

"The increase of surface NH_3 concentrations in eastern China was consistent with the trend of NH_3 emission estimates by a recent study (Zhang et al., 2017). Approximately 85% of the inter-annual variations was due to the changes of human activities, and the remaining 15% resulted from air temperature changes. Agricultural activities is the main drive of NH_3 emission increase, of which 43.1% and 36.4% were contributed by livestock manure and fertilizer application (Zhang et al., 2017).".

Response to Referee #2

We thank the reviewer very much for the detailed and valuable comments. We believe that addressing the issues raised by the reviewer will considerably improve the quality of our manuscript. Please see our response to each comment below (in blue).

Received and published: 13 May 2019

This is a useful, but also rather coarse and preliminary, study using IASI satellite retrievals to provide information about surface NH_3 concentrations and trends. The study uses coarse resolution GEOS-Chem vertical profile information with column information retrieved from IASI. Overall there is convincing correspondence of the IASI retrievals with surface concentrations, although more robust statistical analysis beyond showing correlation and bias is precluding understanding how good (or bad) the correspondence really is. How many observations were within a factor of two of the satellite derived values, is there a difference between rural, semi-urban, urban values, etc.

Thanks very much for this comment. We have added the following text for clarifications in the section of "Validation of satellite-derived surface NH_3 concentrations":

"Overall, 72.85% of observations (including China, the US and Europe) were within a factor of two of the satellite-derived surface NH_3 concentrations. In China, there is approximately 71.43% and 77.27% of observations were within a factor of two of the satellite-derived surface NH_3 concentrations in urban and rural land uses, respectively. There is no big difference in the accuracy of satellite-derived surface NH_3 concentrations between urban and rural land uses. In the US, the monitoring sites were generally distributed at rural sites (http://www.radiello.com) (Li et al., 2016), and, in Europe, there is no information to indicate the land use of each site (https://projects.nilu.no//ccc/) (Tørseth et al., 2012)."

One of the issues that have always remained a bit of mystery to me with regard to the satellite retrievals is the importance of using a-priori profile information for the

retrievals, given the lack of sensitivity close to the surface and possibly also saturation effects where concentrations are high. This paper adds another question mark: when on the one hand the retrieval uses profile information, and in a second step the method uses the same model to calculate surface information is there a potential for using twice the same information?

We have added the following text for more clarifications (the purposes of using the profiles twice were different) in Sect. "IASI NH_3 measurements":

"The ANNI-NH3-v2.2R-I datasets used the ANNI algorithm and took account of the influence of the NH_3 vertical profiles, pressure, humidity and temperature profiles, which was to make the columns accurate. There is no information on NH_3 vertical profiles in the ANNI-NH3-v2.2R-I datasets. The NH_3 vertical profiles used in this paper was to convert the columns to surface concentrations and to make the surface NH_3 estimates accurate.".

Also unclear to me how the vertical resolution of GEOSCHEM can resolve the strong vertical gradients that are likely to exist in source regions. The authors should indicate 1) the vertical structure of the model, 2) the measurement characteristics of the surface observation (including height), 3) how this information is used to calculate surface concentrations. Even if the authors will not resolve all issues, a thorough discussion and way-forward discussion are needed about this.

Thanks very much for this good comment. We have added the following text for clarifications:

"The IASI NH_3 data we gained are column data, and there is no information on the vertical information. To convert this columns to surface concentrations, we used the widely used modelled vertical profiles from GEOS-Chem. The GEOS-Chem outputs include 47 layers, which are not continuous in the vertical direction. To gain the continuous vertical NH_3 profile, we used the Gaussian function to fit the 47 layers' NH_3 concentrations. The main advantage to simulate the vertical profiles is that the NH_3 concentration at any height indicated by satellite can be obtained. On the other hand, the simulated profile function has a general rule, which can convert the columns

indicated by satellite to surface concentration simply and quickly."

The GEOS-Chem can simulate the NH_3 vertical profiles at 47 layers, and can simulate NH_3 concentrations at each layer (from approximately 50 m to 20000 m). Most of all the sites in China, US and Europe were set a height of 1-50 m above the ground (Xu et al., 2015;Li et al., 2016). Please note that the height that we mean here is the height to the ground rather than the height above sea level.

For these reasons I recommend major revisions to his paper.

I would ask the authors to already put on-line the vertical model information for use by other readers.

Thanks very much for this good suggestion. We added the NH_3 vertical model information (Matlab code) as the supporting materials in this revision.

Detailed comments

l. 24 Not only for dry deposition, also for modelling of the formation of ammonium nitrate.

We have added it as suggested.

l. 32: I am wondering what a high correlation of satellite/surface obs taken all regions together is really telling? I think it mostly depends on getting the levels of the 'high' concentrations correct, which is confirmed by the numbers given later. Consider removing this statement.

This indicates the overall accuracy assessment of satellite-based estimates compared with all observations, which include not only "high" concentrations but also "low" concentrations.

l. 65. They have not been established to measure NH_3 by itself, but as one of the parameters of a larger range of pollutants.

We have changed it as suggested.

l. 110 -116. It seems a selling point to suggest that vertical profile information for NO_2 and SO_2 have been useful for modelling, and therefore also for NH_3. The issues is more complex for NH_3, with sources almost entirely close to the surface, and a

complex mix of source and sinks, which will make the model profile more dependent on the mixing characteristics of the CTM. For NO_2 and SO_2 the sources and locations are better known, most of SO_2 is nowadays emitted also well above the surface, which makes interference with the dry deposition process less sensitivity to errors.

We agree with you that there are different sources and sinks between NH_3, NO_2 and SO_2. There is no causal relationship of using vertical profile information for NO_2, SO_2 as well as for NH_3. IASI-derived surface NH_3 concentrations combining NH_3 vertical profiles from CTMs in China and Europe were evaluated previously (Liu et al., 2017;Graaf et al., 2018). Following these studies, the aim of this paper is to determine for the applicability and the assessment of using IASI retrievals and the vertical profile for global surface NH_3 concentrations. Our results shows that the satellite-based approach achieved a high predictive power for annual surface NH_3 concentrations compared with the measurements of all sites in China, US and Europe (R^2=0.76 and RMSE=1.50 μg N m^{-3}).

l. 134: GEOSCHEM vertical profiles were used in the retrieval and subsequently used to derive surface concentrations=>explain

We have added the following text for more clarifications in Sect. "IASI NH_3 measurements":

"The ANNI-NH3-v2.2R-I datasets used the ANNI algorithm and took account of the influence of the NH_3 vertical profiles, pressure, humidity and temperature profiles, which was just to make the columns accurate. There is no information on NH_3 vertical profiles in the ANNI-NH3-v2.2R-I datasets. The NH_3 vertical profiles used in this paper was to convert the columns to surface concentrations and to make the surface NH_3 estimates accurate.".

l. 147. Please summarize some characteristics. E.g. error statistics, characteristic of sites (urban, rural, vicinity to direct sources) height of observations.

We have added the following text for clarifications in the section of "Surface NH_3 measurements":

"In China, we used the national measurements from the Chinese Nationwide Nitrogen

Deposition Monitoring Network (NNDMN) including 10 urban sites, 22 rural sites, and 11 background sites.

The precision for monthly measurements at a site using DELTA systems is as below approximately 10% (Sutton et al., 2001), the correlation between the ALPHA and DELTA measurements was highly significant (R^2=0.919, p<0.001) (Xu et al., 2015).

Surface NH_3 concentrations in the AMoN-US were measured by the radiello diffusive sampler (http://www.radiello.com) as a simple diffusion-type sampler collected every 2 weeks, and these sites were generally distributed at rural sites (Li et al., 2016).

The overall bias of the different instruments in EMEP varied from -30 to 10% for all sites (Bobrutzki et al., 2010). Most of all the sites in China, US and Europe were set a height of 1-50 m above the ground (Xu et al., 2015;Li et al., 2016;Puchalski et al., 2011).".

l. 153 Need to explain why temporal averaging to 2 weeks is done.

We have added the following text for clarification:

"Surface NH_3 concentrations in the AMoN-US were measured by the radiello diffusive sampler (http://www.radiello.com) as a simple diffusion-type sampler collected every 2 weeks (Li et al., 2016). We calculated annual surface NH_3 concentrations by averaging all the measurements since we compared the measured surface NH_3 concentrations with satellite-derived surface NH_3 concentrations on a yearly scale.".

l. 157 measured systems=>measurement systems

We have replaced "measured systems" with "measurement systems".

l. 164 Please give the characteristic heights of the layers in the boundary (mixing) layer.

We have added the following text in the caption of Fig. S4 to show more information:

"The middle height of 1, 10, 20, 30 and 40 layer was approximately 60, 700, 2000, 6000 and 10000 m, respectively.".

l. 160 Any spin-up considered?

Yes, we have added the following text for clarifications:

"We have done the spin up for 5 months, which well exceed the typical lifetime of atmospheric NH_3 (typically within 24 hours) and aerosol ammonium ions (typically within a week) (Pye et al., 2009).".

l. 174: how does this compare to the widely used HTAP2 emissions for 2010? What changes to EDGAR result from substituting with regional inventories. Any seasonality applied and what would be the reference for it?

HTAP v2.2 is constructed by harmonizing regional emission inventories from USA, Canada, Europe and Asia, and gap-filling the rest of the world by EDGAR v4.3 (Janssens-Maenhout et al., 2015), which is methodologically consistent with our emission configuration. We compared the emissions from EDGAR v4.2 with HTAP v2.2 at 2008, which have differences in global total NH_3 within 10% (Crippa et al., 2018). The main difference between the regional inventories and EDGAR is that seasonality of emissions is included in regional inventories,. The seasonality of the regional emissions inventories is embedded as integral part of the inventory except EMEP (Janssens-Maenhout et al., 2015;Crippa et al., 2018;Lenhart and Friedrich, 1995). We have added the above explanations in the section of "GEOS-Chem model".

l. 186 some clarification is need as regards the use of 'local' times, which I think are not considering any shift in legal times (i.e. winter/summertime).

We have added the following text for more clarification, and there is no need to consider shift in legal times:

"The local time is the time in a particular region or area expressed with reference to the meridian passing through it.".

l. 206. It is not clear why this more complex fitting procedure is needed. What was the problem, and how is solved by this new fitting. In figure S2 vertical profiles are shown but I do not have the information to understand if GEOSCHEMs vertical resolution would be able to resolve such profiles.

Please refer to the first paragraph in the section of "Estimation of surface NH_3 concentrations. The IASI NH_3 data we gained are column data, and there is no information on the vertical information. To convert the columns to surface

concentrations, we used the widely used modelled vertical profiles from GEOS-Chem. The GEOS-Chem outputs include 47 layers, which are not continuous in the vertical direction. To gain the continuous vertical NH_3 profile, we used the Gaussian function to fit the 47 layers' NH_3 concentrations. The main advantage to simulate the vertical profiles is that the NH_3 concentration at any height indicated by satellite can be obtained. On the other hand, the simulated profile function has a general rule, which can convert the columns indicated by satellite to surface concentration simply and quickly.

l. 223 like mentioned earlier, the correlation is merely due to the fact of having very high concentrations in one region, versus low in other regions. If one would compare the low concentration range a factor of 5 or so difference in concentrations belong to a single column value would be found. And maybe in reality even more, depending on a whole lot of things.

We agree with you that, on a local scale, the relationship of surface NH_3 concentrations and NH_3 columns may be affected by many factors. Here we show the overall accuracy assessment on a global scale between the surface NH_3 concentrations and NH_3 columns based on the GEOS-Chem outputs, which include not only "high" concentrations but also "low" concentrations.

l. 234 also this seems to be a rather error sensitive approach. I am mostly concerned about possible co-variance between the intra-day emission variations and the limited sampling at 9 O'clock. Are there observations that can be used to explore this issue?

No, we donot have observations to validate the intra-day emission variations.

L 242 Something wrong with reference E et al. And Van et al. And maybe other references as well.

We have corrected all these references.

l. 241-249 I am confused about the Figure S1 (with typical maxima of about 20-40 meter) and the statement that models and aircraft measurements can be used to verify them. I think that high towers like the one at Cabouw (NL), and observations at several levels, are probably the more reliable verification, but unfortunately there are

not many of these.

Fig. S1 just show an example of a possible NH_3 vertical profile, and the typical maxima can be any height such as 20 m, 200 m or other values. In the future we hope to have more aircraft measurements to validate the simulations.

L 250 I have no idea what heights the first and fifth layer are corresponding to.

We have added the following text in the caption of Fig. S3 to show more information: "The middle height of first and fifth layer was approximately 60 m and 340 m, respectively.".

l. 284 It is true that NH_3 can be more accurately be retrieved in one region than another depending on the thermal contrast. But it is not clear to me why this would be so much better in China than e.g. in the US? I guess it is also just a matter of detection limits? It could also be related to more reliable simulation of mixing, depending on sufficient observational input into the parent weather model.

We agree with you that the accuracy of IASI-retrieved surface NH_3 concentrations in different regions is highly linked with the thermal contrast (TC) and the simulation of NH_3 mixing from GEOS-Chem. We have added the following text to discuss the potential reasons.

"The accuracy of IASI-retrieved surface NH_3 concentrations in different regions is highly linked with the thermal contrast (TC) and atmosphere NH_3 abundance (Whitburn et al., 2016). The lowest uncertainties occurred when high columns and high TC coincide. In case either of them decrease, the uncertainty will gradually increase. In case both the TC and column are low, all sensitivity to NH_3 is lost. When high TC and high NH_3 columns (high HRI) occurs, the major contribution to the uncertainty results from the thickness of the NH_3 layer, the surface temperature as well as the temperature profile (Whitburn et al., 2016). In addition, the simulation of NH_3 mixing from GEOS-Chem may have different accuracy in different regions, and thus can cause uncertainty to the different accuracy of IASI-retrieved surface NH_3 concentrations in different regions.".

l. 296 the fixed profiles=>fixed profiles (language)

We have corrected it as suggested.

l. 304-312 I believe that there can be a large difference between 40-60 meters, but as the authors explain this is all in the same geos-chem layer. I fail to understand how this information is then used to interpret geos-chem profiles.

We used the equation (2) to fit NH_3 vertical profiles at each grid box by the following equation (Liu et al., 2017):

$$\rho = \sum_{i=1}^{n} \rho_{max,i} e^{-(\frac{Z-Z_{0,i}}{\sigma_i})^2} \quad (2)$$

Once the NH_3 vertical profiles were determined at each grid box, we can extrapolate NH_3 concentrations at any height from the GEOS-Chem ($G_{GEOS-Chem}$).

Then we can calculate the IASI-derived NH_3 concentrations any height using the NH_3 vertical profiles and IASI NH_3 columns:

$$\overline{G_{IASI_{9-10}}} = \frac{G_{GEOS-Chem}}{\Omega_{GEOS-Chem}} \times \overline{\Omega_{IASI_{9-10}}} \quad (3)$$

where $\overline{G_{IASI_{9-10}}}$ is the satellite-derived surface NH_3 concentrations at a GEOS-Chem grid size at 9-10am; $\frac{G_{GEOS-Chem}}{\Omega_{GEOS-Chem}}$ is the ratio of surface NH_3 concentrations to NH_3 columns calculated from GEOS-Chem; $\overline{\Omega_{IASI_{9-10}}}$ is the average IASI NH_3 columns at a GEOS-Chem grid at 9-10am.

All the information has been described in detail in the method section.

l. 323 this is mostly a confirmation that crop mask used by the regional and global emission inventories correspond to the MODIS one. And that the fertilizers used in those countries indeed end up on these fields.

Yes, it is.

l. 355 According to inventories, in Europe about 20 % of NH_3 emissions is related to the use of mineral fertilizer, and 80 % to manure managements. So it would be more relevant to determine the correspondence of those emissions (mineral is often used to top up what wasn't provided by manure).

Thank you very much for this suggestion. We have carefully checked the NH_3 emissions in Europe. According to Emissions Database for Global Atmospheric Research (EDGAR), in western Europe, manure management accounts for 53% and

the share of emissions from agricultural soils for 43% of the ammonia emissions. So we have added the N manure into our analysis in Fig. 4 and Fig. 5 and revised related text in the discussion.

364 Van et al. Please check this reference. It seems to be a problem of your reference manager.

We have checked this reference, and revised it.

370 It is probably opportune to refer to the paper by Pozzer et al, a 1x1 model study that has more extensively studied the role of NH_3 emission for aerosol. It is also important to critically assess ammonium nitrate measurements, which are notoriously difficult at higher concentrations. Would it be an option to use the model to estimate (equilibrium) ammonium sulfate and nitrate concentrations associated with the 'retrieved' surface ammonia?

We have carefully read the suggested paper on the the role of NH_3 emission for aerosol (Pozzer et al., 2012). We agree with the reviewer that it is important to assess ammonium nitrate measurements associated with the retrieved surface NH_3 concentrations. However, this has been out of the scope of this paper, and this paper focuses on the estimates of surface NH_3 concentrations inferred from satellite retrievals. It is more appropriate to estimate ammonium sulfate and nitrate concentrations in another paper in the future.

421-430 Biomass burning can be an important source of NH_3, especially in the smoldering phase. Therefore, I have some doubts that active fire products are the best proxy for NH_3 emission. Did you consider burnt area products instead?

We here compared the monthly variations of surface NH_3 concentrations and biomass burning. The MODIS active fires are considered to be more accurate than the burnt area products on the timing of burning. Please see the temporal intercomparison of burned area products with Active Fire data set (Humber et al., 2019).

activity leaded=>led?

We have replaced "leaded" with "led".

504: why inconsistent? It could be rather consistent, as you explain in the following

sentences.

We have added the following text to explain this inconsistency:

"This inconsistency between NH_3 and NO_x trends in the US was mainly due to different emission control policies. Over the past two decades, due to the implementation of effective regulations and emission reduction measures for NO_x, the NO_x emission in the US decreased by nearly 41% between 1990 and 2010 (Hand et al., 2014). However, this NH_3 increase in eastern US is likely due to the lack of NH_3 emission control policy as well as the decreased NH_3 removal due to the decline in acidic gases (NO_2 and SO_2) (Warner et al., 2017;Li et al., 2016).".

Supplementary

Figure S3: Please indicate what heights approximate correspond with the first and fifth layer boundaries.

We have added the following text in the figure caption:

"The middle height of first and fifth layer was approximately 60 m and 340 m, respectively.".

Figure S4: no idea what heights these layer correspond to.

We have added the following text in the figure caption:

"The middle height of 1, 10, 20, 30 and 40 layer was approximately 60, 700, 2000, 6000 and 10000 m, respectively.".

Figure S5: the figure caption is not self-explaining.

We have revised the figure caption by the following text to better describe the figure:

"Difference of surface NH_3 concentrations between 40m and 60m.".

Figure S6: first PM2.5 and then NO_2 in caption.

We have corrected it in the caption to match it with the figure.

Figure S9: describe upper panel as well.

We have added the following text to describe the panel:

"The upper panel is the annual raw fire counts in 2014.".

Figure S10: trends of what (annual concentrations?) and for what period

Yes, it is annual concentration during 2008-2016. We have changed the original descriptions by the following text:

"…trends of annual surface NH_3 concentrations during 2008-2016".

Reference

Bobrutzki, K. V., Braban, C. F., Famulari, D., Jones, S. K., Blackall, T., Smith, T. E. L., Blom, M., Coe, H., Gallagher, M., and Ghalaieny, M.: Field inter-comparison of eleven atmospheric ammonia measurement techniques, Atmospheric Measurement Techniques,3,1(2010-01-27), 2, 91-112, 2010.

Crippa, M., Guizzardi, D., Muntean, M., Schaaf, E., Dentener, F., van Aardenne, J. A., Monni, S., Doering, U., Olivier, J. G. J., Pagliari, V., and Janssens-Maenhout, G.: Gridded emissions of air pollutants for the period 1970–2012 within EDGAR v4.3.2, Earth Syst. Sci. Data, 10, 1987-2013, 10.5194/essd-10-1987-2018, 2018.

Graaf, S. C. v. d., Dammers, E., Schaap, M., and Erisman, J. W.: How are NH_3 dry deposition estimates affected by combining the LOTOS-EUROS model with IASI-NH3 satellite observations?, Atmospheric Chemistry and Physics, 18, 13173-13196, https://doi.org/10.5194/acp-2018-133, 2018.

Hand, J. L., Schichtel, B. A., Malm, W. C., Copeland, S., Molenar, J. V., Frank, N., and Pitchford, M.: Widespread reductions in haze across the United States from the early 1990s through 2011, Atmospheric Environment, 94, 671-679, 2014.

Humber, M. L., Boschetti, L., Giglio, L., and Justice, C. O.: Spatial and temporal intercomparison of four global burned area products, International Journal of Digital Earth, 12, 460-484, 10.1080/17538947.2018.1433727, 2019.

Janssens-Maenhout, G., Crippa, M., Guizzardi, D., Dentener, F., Muntean, M., Pouliot, G., Keating, T., Zhang, Q., Kurokawa, J., Wankmüller, R., Denier van der Gon, H., Kuenen, J. J. P., Klimont, Z., Frost, G., Darras, S., Koffi, B., and Li, M.: HTAP_v2.2: a mosaic of regional and global emission grid maps for 2008 and 2010 to study hemispheric transport of air pollution, Atmos. Chem. Phys., 15, 11411-11432, 10.5194/acp-15-11411-2015, 2015.

Kang, Y., Liu, M., Song, Y., Huang, X., Yao, H., Cai, X., Zhang, H., Kang, L., Liu, X., Yan, X., He, H., Zhang, Q., Shao, M., and Zhu, T.: High-resolution ammonia emissions inventories in China from 1980 to 2012, Atmospheric Chemistry and Physics, 16, 2043-2058, 10.5194/acp-16-2043-2016, 2016.

Lenhart, L., and Friedrich, R.: European emission data with high temporal and spatial resolution, Water Air & Soil Pollution, 85, 1897-1902, 1995.

Li, Y., Schichtel, B. A., Walker, J. T., Schwede, D. B., Chen, X., Lehmann, C. M., Puchalski, M. A., Gay, D. A., and Collett, J. L.: Increasing importance of deposition of reduced nitrogen in the United States, Proceedings of the National Academy of Sciences, 113, 5874-5879, 2016.

Liu, L., Zhang, X., Xu, W., Liu, X., Lu, X., Wang, S., Zhang, W., and Zhao, L.: Ground Ammonia Concentrations over China Derived from Satellite and Atmospheric Transport Modeling, Remote Sensing, 9, 467, 2017.

Potter, P., Ramankutty, N., Bennett, E. M., and Donner, S. D.: Characterizing the Spatial Patterns of Global Fertilizer Application and Manure Production, Earth Interactions, 14, 1-22, 10.1175/2009EI288.1, 2010.

Pozzer, A., de Meij, A., Pringle, K. J., Tost, H., Doering, U. M., van Aardenne, J., and Lelieveld, J.: Distributions and regional budgets of aerosols and their precursors simulated with the EMAC chemistry-climate model, Atmos. Chem. Phys., 12, 961-987, 10.5194/acp-12-961-2012, 2012.

Puchalski, M. A., Sather, M. E., Walker, J. T., Lehmann, C. M. B., Gay, D. A., Johnson, M., and Robarge, W. P.: Passive ammonia monitoring in the United States: comparing three different sampling devices, Journal of Environmental Monitoring, 13, 3156, 2011.

Pye, H. O. T., Liao, H., Wu, S., Mickley, L. J., Jacob, D. J., Henze, D. K., and Seinfeld, J. H.: Effect of changes in climate and emissions on future sulfate-nitrate-ammonium aerosol levels in the United States, Journal of Geophysical Research: Atmospheres, 114, 10.1029/2008jd010701, 2009.

Shen, J. L., Tang, A. H., Liu, X. J., Fangmeier, A., Goulding, K. T. W., and Zhang, F.

S.: High concentrations and dry deposition of reactive nitrogen species at two sites in the North China Plain, Environmental Pollution, 157, 3106-3113, http://dx.doi.org/10.1016/j.envpol.2009.05.016, 2009.

Sutton, M. A., Tang, Y. S., Miners, B., and Fowler, D.: A New Diffusion Denuder System for Long-Term, Regional Monitoring of Atmospheric Ammonia and Ammonium, Water Air & Soil Pollution Focus, 1, 145-156, 2001.

Tørseth, K., Aas, W., Breivik, K., Fjæraa, A. M., Fiebig, M., Hjellbrekke, A. G., Lund Myhre, C., Solberg, S., and Yttri, K. E.: Introduction to the European Monitoring and Evaluation Programme (EMEP) and observed atmospheric composition change during 1972–2009, Atmos. Chem. Phys., 12, 5447-5481, 10.5194/acp-12-5447-2012, 2012.

Van Damme, M., Clarisse, L., Dammers, E., Liu, X., Nowak, J., Clerbaux, C., Flechard, C., Galy-Lacaux, C., Xu, W., and Neuman, J.: Towards validation of ammonia (NH_3) measurements from the IASI satellite, Atmospheric Measurement Techniques, 7, 12125-12172, 2014.

Van Damme, M., Erisman, J. W., Clarisse, L., Dammers, E., Whitburn, S., Clerbaux, C., Dolman, A. J., and Coheur, P. F.: Worldwide spatiotemporal atmospheric ammonia (NH_3) columns variability revealed by satellite, Geophysical Research Letters, 42, 8660-8668, 2015.

Warner, J. X., Dickerson, R. R., Wei, Z., Strow, L. L., Wang, Y., and Liang, Q.: Increased atmospheric ammonia over the world's major agricultural areas detected from space, Geophysical Research Letters, 10.1002/2016GL072305, 2017.

Whitburn, S., Van Damme, M., Clarisse, L., Bauduin, S., Heald, C. L., Hadji-Lazaro, J., Hurtmans, D., Zondlo, M. A., Clerbaux, C., and Coheur, P. F.: A flexible and robust neural network IASI-NH_3 retrieval algorithm, Journal of Geophysical Research: Atmospheres, 121, 6581-6599, 10.1002/2016JD024828, 2016.

Xu, W., Luo, X. S., Pan, Y. P., Zhang, L., Tang, A. H., Shen, J. L., Zhang, Y., Li, K. H., Wu, Q. H., Yang, D. W., Zhang, Y. Y., Xue, J., Li, W. Q., Li, Q. Q., Tang, L., Lv, S. H., Liang, T., Tong, Y. A., Liu, P., Zhang, Q., Xiong, Z. Q., Shi, X. J., Wu, L. H., Shi, W.

Q., Tian, K., Zhong, X. H., Shi, K., Tang, Q. Y., Zhang, L. J., Huang, J. L., He, C. E., Kuang, F. H., Zhu, B., Liu, H., Jin, X., Xin, Y. J., SHi, X. K., Du, E. Z., Dore, A. J., Tang, S., Collett Jr, J. L., Goulding, K., Sun, Y. X., Ren, J., Zhang, F. S., and Liu, X. J.: Quantifying atmospheric nitrogen deposition through a nationwide monitoring network across China, Atmospheric Chemistry and Physics, 15, 12345-12360, 2015.

Zhang, X., Wu, Y., Liu, X., Reis, S., Jin, J., Dragosits, U., Van Damme, M., Clarisse, L., Whitburn, S., Coheur, P.-F., and Gu, B.: Ammonia Emissions May Be Substantially Underestimated in China, Environmental Science & Technology, 51, 12089-12096, 10.1021/acs.est.7b02171, 2017.

Estimating global surface ammonia concentrations inferred from satellite retrievals

Lei Liu [a, b, c] , Xiuying Zhang [b, *], Anthony Y.H. Wong [c], Wen Xu [d], Xuejun Liu [d], Yi Li [e], Huan Mi [c, f], Xuehe Lu [b], Limin Zhao [b], Zhen Wang [b], Xiaodi Wu [b, g], Jing Wei [h]

[a] College of Earth and Environmental Sciences, Lanzhou University, Lanzhou 730000, China

[b] International Institute for Earth System Science, Nanjing University, Nanjing, 210023, China

[c] Department of Earth and Environment, Boston University, Boston, Massachusetts, USA

[d] College of Resources and Environmental Sciences, Centre for Resources, Environment and Food Security, Key Lab of Plant-Soil Interactions of MOE, China Agricultural University, Beijing, 100193, China

[e] Sunset CES Inc., Beaverton, OR, 97008, USA

[f] College of Surveying and Geo-Informatics, Tongji University, 1239 Siping Road, Shanghai, China

[g] Jiangsu Center for Collaborative Innovation in Geographical Information Resource Development and Application, Nanjing, 210023, China

[h] College of Global Change and Earth SystemScience, Beijing Normal University, Beijing, China,

* Correspondence to Xiuying Zhang (zhangxy@nju.edu.cn).

Abstract

Ammonia (NH_3), as an alkaline gas in the atmosphere, can cause direct or indirect effects on the air quality, soil acidification, climate change as well as human health. Estimating surface NH_3 concentrations is critically important for modelling the dry deposition of NH_3 and for modelling the formation of ammonium nitrate, which have important impacts on the natural environment. However, sparse monitoring sites make

it challenging and difficult to understand the global distribution of surface NH_3 concentrations both in time and space. We estimated the global surface NH_3 concentrations for the years of 2008-2016 using the satellite NH_3 retrievals combining its vertical profiles from the GEOS-Chem. The accuracy assessment indicates that the satellite-based approach has achieved a high predictive power for annual surface NH_3 concentrations compared with the measurements of all sites in China, US and Europe (R^2=0.76 and RMSE=1.50 μg N m^{-3}). The satellite-derived surface NH_3 concentrations had higher consistency with the ground-based measurements in China (R^2=0.71 and RMSE=2.6 μg N m^{-3}) than the US (R^2=0.45 and RMSE=0.76 μg N m^{-3}) and Europe (R^2=0.45 and RMSE=0.86 μg N m^{-3}) at a yearly scale. Annual surface NH_3 concentrations higher than 6 μg N m^{-3} are mainly concentrated in the North China Plain of China and Northern India, followed by 2-6 μg N m^{-3} mainly in southern and northeastern China, India, western Europe and eastern United States (US). High surface NH_3 concentrations were found in the croplands in China, US and Europe, and surface NH_3 concentrations in the croplands in China were approximately double than those in the croplands in the US and Europe. The linear trend analysis shows that an increase rate of surface NH_3 concentrations (>0.2 μg N m^{-3} y^{-1}) appeared in the eastern China during 2008-2016, and a middle increase rate (0.1-0.2 μg N m^{-3} y^{-1}) occurred in northern Xinjiang over China. NH_3 increase was also found in agricultural regions in middle and eastern US with an annual increase rate of lower than 0.10 μg N m^{-3} y^{-1}. The satellite-derived surface NH_3 concentrations help us to determine the NH_3 pollution status in the areas without monitoring sites and to estimate the dry deposition of NH_3 in the future.

Introduction

Ammonia (NH_3), emitted primarily by agricultural activities and biomass burning, is an important alkaline gas in the atmosphere (Van Damme et al., 2018;Warner et al., 2017). Excessive surface NH_3 concentrations can cause chronic or acute damage to the plant (such as reduced growth and bleached gray foliage) when its capacity of detoxification is exceeded (Eerden, 1982;Sheppard et al., 2008). Estimation of surface

NH_3 concentrations is critically important in modelling the dry deposition of NH_3, which may comprise a large part of atmospheric nitrogen (N) deposition, and could cause acidification in the soil, eutrophication in the aquatic ecosystems, and contamination in drinking water (Basto et al., 2015;Kim et al., 2014;Lamarque et al., 2005;Larssen et al., 2011;Reay et al., 2008). In addition, NH_3 can also react with nitric acid and sulfuric acid to form ammonium salts (Li et al., 2014;Li et al., 2017b), which are important components of particulate matters (PM), and have negative impacts on air quality and human health (Xu et al., 2017;Schaap et al., 2004).

Several national monitoring programs can measure surface NH_3 concentrations, including the Chinese Nationwide Nitrogen Deposition Monitoring Network (NNDMN) established in 2004, the Ammonia Monitoring Network in China (AMoN-China) established in 2015 in China, the Ammonia Monitoring Network in the US (AMoN-US) as well as the European Monitoring and Evaluation Programme (EMEP). However, there are still relatively large uncertainties of estimating global surface NH_3 concentrations, resulting from the sparse monitoring sites as well as the limited spatial representativeness (Liu et al., 2017b;Liu et al., 2017a). Satellite NH_3 retrievals are an important complement to gain the global distribution of NH_3 concentrations with a high spatial resolution (Van Damme et al., 2014c). NH_3 can be measured by several satellite instruments including the Infrared Atmospheric Sounding Interferometer (IASI), Atmospheric Infrared Sounder (AIRS), Cross-track Infrared Sounder (CrIS) and Tropospheric Emission Spectrometer (TES). TES using the thermal infrared spectral range has sparser spatial coverage compared to IASI, CrIS and AIRS (Shephard et al., 2011;Zhang et al., 2017a). A recent study (Kharol et al., 2018) reported the dry NH_3 depositions in North America, and found -15% underestimation in CrIS surface NH_3 concentrations (using three fixed NH_3 profiles considering unpolluted, moderate and polluted conditions) compared with the measurements from the AMoN-US during the warm months (from April to September). Warner et al. reported the global AIRS NH_3 concentrations at 918hPa (approximately 700-800 m) at 1° latitude $\times$ 1° longitude grids, and found NH_3 concentrations increased in the major agricultural regions during 2003-2015 (Warner

et al., 2017). The IASI NH_3 measurements have been validated with NH_3 columns measured by the Fourier transform infrared spectroscopy (FTIR), ground-based NH_3 measurements, NH_3 emissions and atmospheric chemistry transport models (CTMs) (Dammers et al., 2016;Van Damme et al., 2014c;Van Damme et al., 2014a;Whitburn et al., 2016).

Apart from satellite retrievals, CTMs are also powerful tools to investigate spatiotemporal variability of surface NH_3 concentrations in the atmosphere. Schiferl et al. evaluated the modelled NH_3 concentrations during 2008-2012 from GEOS-Chem, and found an approximately 26% underestimation compared with the ground-based measurements, which can be related to the relatively large uncertainties in NH_3 emissions used for driving GEOS-Chem (Schiferl et al., 2015). Zhu et al. used the GEOS-Chem constrained by TES measurements to estimate surface NH_3 concentration during 2006-2009, and found an improvement in comparison with the ground-based measurements in the United States (Zhu et al., 2013). Schiferl et al. used the airborne observations to validate the simulated NH_3 concentrations in 2010 from GEOS-Chem, and revealed reasonably simulated NH_3 vertical profiles compared with the aircraft measurements but with an underestimation in surface NH_3 concentrations in California (Schiferl et al., 2014). A number of previous studies have used satellite NO_2 columns to estimate the surface NO_2 concentrations combining NO_2 vertical profiles from CTMs (Geddes et al., 2016;Lamsal et al., 2013;Nowlan et al., 2014;Liu et al., 2017c). The methods of using the vertical profiles to convert satellite-retrieved columns to surface concentrations have been proven successful for SO_2 and NO_2 (Geddes et al., 2016;Geng et al., 2015;Lamsal et al., 2008;Nowlan et al., 2014). CTMs can provide valuable information of NH_3 vertical profiles (Whitburn et al., 2016;Liu et al., 2017b), and IASI-derived surface NH_3 concentrations combining NH_3 vertical profiles from CTMs in China and Europe were evaluated previously (Liu et al., 2017b;Graaf et al., 2018). This study followed these studies to estimate the satellite-derived global surface NH_3 concentrations using IASI NH_3 retrievals and the vertical profiles from GEOS-Chem, and the present study aims to estimate the global surface NH_3 concentration from a satellite perspective.

Data and Methods

IASI NH_3 measurements

The Infrared Atmospheric Sounding Interferometer (IASI) is a passive instrument measuring infrared radiation within the spectral range of 645-2769 cm^{-1}. The IASI-A instrument is on board of the MetOp-A satellite launched in 2006 covering the globe twice a day with an elliptical spatial resolution of approximately 12 by 12 kilometers, and cross the equator at 09:30 and 21:30 local times (Van Damme et al., 2014b). We used the daytime IASI NH_3 measurements due to the larger positive thermal contrast detected by satellite instruments leading to smaller errors compared to the nighttime data (Van Damme et al., 2014b). In this work, we used the IASI NH_3 columns products (ANNI-NH3-v2.2R-I) during 2008-2016 (Van Damme et al., 2017) to estimate the global surface NH_3 concentrations. The ANNI-NH3-v2.2R-I datasets were developed by converting spectral HRI (hyperspectral range index) to NH_3 columns through an Artificial Neural Network for IASI (ANNI) algorithm (Whitburn et al., 2016). This algorithm considered the influence of the NH_3 vertical profiles, pressure, humidity and temperature profiles. The NH_3 vertical profile information used to generate the ANNI NH_3 columns were retrieved from GEOS-Chem, which integrates H_2SO_4-HNO_3-NH_3 aerosol thermodynamics mechanism (Whitburn et al., 2016;Van Damme et al., 2017). The ANNI-NH3-v2.2R-I datasets used the ANNI algorithm and took account of the influence of NH_3 vertical profiles, pressure, humidity and temperature profiles, which was to make the columns accurate. There is no information on NH_3 vertical profiles in the ANNI-NH3-v2.2R-I datasets. The NH_3 vertical profiles used in this paper was to convert the columns to surface concentrations and to make the surface NH_3 estimates accurate. The IASI NH_3 columns used in this study were processed into the monthly data at 0.25 ° latitude × 0.25 ° longitude grids by the arithmetic averaging method (Van Damme et al., 2017;Whitburn et al., 2016;Liu et al., 2017a).

Surface NH_3 measurements

To evaluate our satellite-derived global surface NH_3 concentrations, we collected available surface NH_3 measurements on a regional scale in 2014. In China, we used the national measurements from the Chinese Nationwide Nitrogen Deposition Monitoring Network (NNDMN) including 10 urban sites, 22 rural sites, and 11 background sites. Surface NH_3 concentrations in the NNDMN were measured by both ALPHA (Adapted Low-cost, Passive High Absorption) and DELTA (Denuder for Long-Term Atmospheric sampling) systems. The bias for monthly measurements at a site using DELTA systems is as below approximately 10% (Sutton et al., 2001), and the correlation between the ALPHA and DELTA measurements was highly significant (R^2=0.919, p<0.001) (Xu et al., 2015). The detailed descriptions on the NNDMN have been described in a previous study (Xu et al., 2015). In the US, we used the measurements of 67 sites from the AMoN-US, downloaded from the website: http://nadp.sws.uiuc.edu/AMoN/. Surface NH_3 concentrations in the AMoN-US were measured by the radiello diffusive sampler (http://www.radiello.com) as a simple diffusion-type sampler collected every 2 weeks, and these sites were generally distributed at rural sites (Li et al., 2016). We calculated annual surface NH_3 concentrations by averaging all the measurements since we compared the measured surface NH_3 concentrations with satellite-derived surface NH_3 concentrations at a yearly scale. In Europe, we used the measurements of 43 sites from the EMEP network (https://www.nilu.no/projects/ccc/emepdata.html). The EMEP is composed of multiple national networks in Europe, thus the measurement systems differs among different national networks. The overall bias of the different instruments in EMEP varied from -30 to 10% for all sites (Bobrutzki et al., 2010). Most sites in China, US and Europe were set a height of 1-50 m above the ground (Xu et al., 2015;Li et al., 2016;Puchalski et al., 2011).

GEOS-Chem model

We used GEOS-Chem version 11-01 as the chemical transport model to calculate

global NH_3 vertical profiles (using the year of 2014 as a case study in the results and discussion). We did the spin up for 5 months, which well exceed the typical lifetime of atmospheric NH_3 (typically within 24 hours) and aerosol ammonium ions (typically within a week) (Pye et al., 2009). It has a spatial resolution of 2 ° latitude × 2.5 ° longitude × 47 vertical layers spanning over Earth's surface and about 80 km above it. It is driven by the meteorological field data of the GEOS-FP (forward-processing) products, which were produced by NASA GMAO (Global Modelling and Assimilation Office) (https://gmao.gsfc.nasa.gov/). Here we modelled the NH_3 vertical profiles using GEOS-Chem, and used the monthly averages for analysis. The global NH_3 emissions in GEOS-Chem are based on the EDGAR (Emissions Database for Global Atmospheric Research) v4.2 (http://edgar.jrc.ec.europa.eu/overview.php?v=42), while the regional emissions are replaced with MIX inventory for East Asia (Li et al., 2017a) (http://www.meicmodel.org/dataset-mix.html), EMEP inventory for Europe (http://www.emep.int/), NEI (National Emissions Inventory, 2011) for the US (https://www.epa.gov/air-emissions-inventories) and CAC (Criteria Air Contaminant) inventory for Canada (https://www.canada.ca/en/services/environment/pollution-waste-management/national-pollutant-release-inventory.html). The main difference between the regional inventories and EDGAR is that seasonality of emissions is included in regional inventories. The seasonality of regional emissions inventories is embedded as integral part of the inventory except EMEP (Janssens-Maenhout et al., 2015;Crippa et al., 2018;Lenhart and Friedrich, 1995). The biomass burning emissions are from Global Fire Emissions Database (GFED4) including agricultural fires, wildfire and pre-scribed burning (Giglio et al., 2013). The GEOS-Chem simulates a comprehensive atmospheric NO_x-O_3-VOC-aerosol system (Mao et al., 2013). The thermodynamic equilibrium of NH_3-H_2SO_4-HNO_3 system is simulated by the ISORROPIA II model (Fountoukis and Nenes, 2007;Pye et al., 2009). The modelling of wet deposition is described by a previous study (Liu et al., 2001) with updates from the studies (Amos et al., 2012;Wang et al., 2011). Dry deposition of particles follows

the size-segregated treatment (Zhang et al., 2001) and gaseous dry deposition follows the framework (Wesely, 1989) with updates from a previous study (Wang et al., 1998). We archive the output daily averages of NH_3 concentrations as well as the averages between 9 and 10 am, which corresponds to the local crossing time of IASI (9:30 am). The local time is the time in a particular region or area expressed with reference to the meridian passing through it. The relationship between NH_3 concentration at 9-10 am and the daily averages derived from the GEOS-Chem was used to convert the satellite observed NH_3 column to daily averages (Nowlan et al., 2014).

Estimation of surface NH_3 concentrations

We estimated global surface NH_3 concentrations using the IASI NH_3 columns as well as the GEOS-Chem. We took into account the advantages of IASI NH_3 columns with high spatial resolutions and the GEOS-Chem with vertical profiles. The IASI NH_3 data we gained are column data, and there is no information on the vertical information. To convert the columns to surface concentrations, we used the widely used modelled vertical profiles from GEOS-Chem. The GEOS-Chem outputs include 47 layers, which are not continuous in the vertical direction. To gain the continuous vertical NH_3 profile, we used the Gaussian function to fit the 47 layers' NH_3 concentrations. The main advantage to simulate the vertical profiles is that the NH_3 concentration at any height indicated by satellite can be obtained. On the other hand, the simulated profile function has a general rule, which can convert the columns indicated by satellite to surface concentration simply and quickly for many years. The height of each grid box used here was calculated at the middle height of each layer rather than the top height of each layer. A three-parameter Gaussian function was used to fit NH_3 vertical profiles at each grid box from the GEOS-Chem in the previous studies (Whitburn et al., 2016;Liu et al., 2017b) :

$$\rho = \rho_{max} e^{-(\frac{Z-Z_0}{\sigma})^2} \qquad (1)$$

where ρ is NH_3 concentrations at the layer height Z; ρ_{max} is the maximum NH_3 concentrations at the height z_0; σ is an indicator for the spread or thickness of the

NH_3 concentrations.

This study expanded the equation (1) to fit NH_3 vertical profiles at each grid box by the following equation (Liu et al., 2017b):

$$\rho = \sum_{i=1}^{n} \rho_{max,i} e^{-(\frac{Z-Z_{0,i}}{\sigma_i})^2} \quad (2)$$

where n ranges from 1 to 6. If n equals 1, the equation (2) is the same as the equation (1); if n is greater than 1, the equation (2) is the multiple three-parameters Gaussian items. We determined the value of n that can simulate the NH_3 vertical profiles with best performance at each grid box using the determining coefficients of R-Square (R^2). Once the NH_3 vertical profiles were determined at each grid box, we can extrapolate NH_3 concentrations at any height from the GEOS-Chem ($G_{GEOS-Chem}$).

We then aggregated the IASI NH_3 columns Ω_{IASI} (0.25 ° latitude × 0.25 ° longitude) to the GEOS-Chem grid size $\overline{\Omega_{IASI}}$ (2 ° latitude × 2.5 ° longitude) by the averaging method. We have the following equation (Lamsal et al., 2008):

$$\overline{G_{IASI_{9-10}}} = \frac{G_{GEOS-Chem}}{\Omega_{GEOS-Chem}} \times \overline{\Omega_{IASI_{9-10}}} \quad (3)$$

where $\overline{G_{IASI_{9-10}}}$ is the satellite-derived surface NH_3 concentrations at a GEOS-Chem grid size at 9-10am; $\frac{G_{GEOS-Chem}}{\Omega_{GEOS-Chem}}$ is the ratio of surface NH_3 concentrations to NH_3 columns calculated from GEOS-Chem; $\overline{\Omega_{IASI_{9-10}}}$ is the average IASI NH_3 columns at a GEOS-Chem grid at 9-10am.

We found a high correlation (R=0.96 and p=0.000) between the surface NH_3 concentrations and NH_3 columns based on the GEOS-Chem outputs (**Fig. S1**). Then we used the satellite-derived scaling factor to downscale the satellite-derived surface NH_3 concentrations at a GEOS-Chem grid by using the following ratio:

$$R_{IASI} = \frac{\Omega_{IASI}}{\overline{\Omega_{IASI}}} \quad (4)$$

$$G_{IASI_{9-10}} = \overline{G_{IASI_{9-10}}} \times R_{IASI} \quad (5)$$

where R_{IASI} is the scaling factor. $G_{IASI_{9-10}}$ is the satellite-derived surface NH_3 concentrations at a satellite IASI grid size (0.25 ° latitude ×0.25 ° longitude) at 9-10am.

To convert the instantaneous satellite-derived surface NH_3 concentrations G_{IASI} to

daily average surface NH_3 concentrations, we followed the methods (Nowlan et al., 2014):

$$G_{IASI}{}^{*}=\frac{G_{GEOS-Chem}^{1-24}}{G_{GEOS-Chem}^{9-10}}\times G_{IASI_{9-10}} \quad (6)$$

where $G_{IASI}{}^{*}$ is the daily average surface NH_3 concentrations, and $\frac{G_{GEOS-Chem}^{1-24}}{G_{GEOS-Chem}^{9-10}}$ is the ratio of the GEOS-Chem surface NH_3 concentrations at the daily average to the average of 9-10 am.

Results and Discussion

NH_3 vertical profiles from GEOS-Chem

NH_3 emitted from the surface can be transported horizontally or vertically, and its concentrations may show a certain gradient in the vertical and horizontal directions (Preston et al., 1997;Rozanov et al., 2005). There are generally two types of shapes of NH_3 vertical profiles (**Fig. S2**) from aircraft measurements (Li et al., 2017b;Tevlin et al., 2017) and CTMs (Whitburn et al., 2016;Liu et al., 2017b). One is representative for the vertical profile with maximum NH_3 concentrations at a certain height (z_0>0) and the other is representative for the vertical profile with maximum NH_3 concentrations near the earth surface (z_0=0). In this study, the vertical profiles of NH_3 were fitted based on the 47 layers' outputs by GEOS-Chem in 2014 at a monthly scale. **Fig. S3** shows the spatial distribution of NH_3 concentrations in the first and fifth layers simulated by GEOS-Chem in January 2014. NH_3 concentrations in the fifth layer are significantly lower than those in the first layer, suggesting that NH_3 concentrations decrease with increasing layers (or altitude), especially in NH_3 hotspot regions (such as eastern China, India, western Europe and eastern US). The average difference of NH_3 concentrations between the first and fifth layers on the land is 0.34 μg N m^{-3}. The average NH_3 concentrations in the first and fifth layers in eastern China, India, western Europe and eastern US were 2.76, 7.28, 0.55 and 0.31 μg N m^{-3}, respectively.

To more vividly depict the vertical profiles of NH_3, we show NH_3 vertical

concentrations with cross-section drawn at 37°N in January, 2014 (**Fig. S4**). High NH_3 concentrations are mainly concentrated in the 1-10 layers, and show a significant decrease trend with the increasing altitude, which is consistent with the aircraft measurements (Preston et al., 1997;Lin et al., 2014;Levine et al., 1980;Shephard and Cady-Pereira, 2015;Li et al., 2017b;Tevlin et al., 2017). NH_3 vertical profiles were fitted by Gaussian function (2-6 terms) based on the 47 layers' NH_3 concentrations from the GEOS-Chem, and the fitting accuracy was determined by R^2. We found that the NH_3 vertical profiles on the land between 60 °N and 55 °S can be well modelled using Gaussian function (R^2 higher than 0.90) (**Fig. 1**). Previous studies also found high accuracy using the Gaussian function to simulate the NH_3 vertical profiles in China and globally (Whitburn et al., 2016;Liu et al., 2017b).

Validation of satellite-derived surface NH_3 concentrations

NH_3 vertical profiles were used to convert IASI NH_3 columns to surface NH_3 concentrations. **Fig. 2** shows the IASI-derived global surface NH_3 concentrations on the land at 0.25 ° latitude × 0.25 ° longitude grids in 2014. IASI-derived surface NH_3 concentrations capture the general spatial pattern of surface NH_3 concentrations fairly well in 2014 in regions with relatively intensive monitoring sites (R^2=0.76 and RMSE=1.50 μg N m^{-3} in **Fig. 2 and Fig. 3**). Overall, 72.85% of observations (including China, the US and Europe) were within a factor of two of the satellite-derived surface NH_3 concentrations. In China, there is approximately 71.43% and 77.27% of observations were within a factor of two of the satellite-derived surface NH_3 concentrations in urban and rural land uses, respectively. There is no big difference in the accuracy of satellite-derived surface NH_3 concentrations between urban and rural land uses. In the US, the monitoring sites were generally distributed at rural sites (http://www.radiello.com) (Li et al., 2016), and, in Europe, there is no information to indicate the land use of each site (https://projects.nilu.no//ccc/) (Tørseth et al., 2012a). The overall mean of satellite-derived surface NH_3 concentrations in 2014 at the measured sites was 2.52 μg N m^{-3} and was close to the average of measured surface NH_3 concentrations (2.51 μg N m^{-3}) in 2014.

IASI-derived surface NH_3 concentrations gained higher consistency with the ground-based measurements in China (R^2=0.71 and RMSE=2.6 μg N m^{-3} for 43 sites) than the US (R^2=0.45 and RMSE=0.76 μg N m^{-3} for 67 sites) and Europe (R^2=0.45 and RMSE=0.86 μg N m^{-3} for 43 sites) at a yearly scale. This might be due to the fact that for high concentrations in a region (associated with high thermal contrast) can be more reliably detected by IASI (Van Damme et al., 2014a). The accuracy of IASI-retrieved surface NH_3 concentrations in different regions is highly linked with the thermal contrast (TC) and atmosphere NH_3 abundance (Whitburn et al., 2016). The lowest uncertainties occur when high columns and high TC coincide. In case either of them decrease, the uncertainty will gradually increase. In case both the TC and column are low, all sensitivity to NH_3 is lost. When high TC and high NH_3 columns (high HRI) occurs, the major contribution to the uncertainty results from the thickness of the NH_3 layer, the surface temperature as well as the temperature profile (Whitburn et al., 2016). The simulation of NH_3 mixing from GEOS-Chem may also have different accuracy in different regions, and thus can cause uncertainty to the different accuracy of IASI-retrieved surface NH_3 concentrations in different regions. Notably, we compared the surface NH_3 concentrations at the monitoring stations with the grid values of satellite-derived estimates directly. This point-to-grid verification strategy may cause uncertainty since the monitoring site location may not be representative of a given grid cell for an average retrieved value. The satellite-derived NH_3 has a detection limit of 0.0025 μg N m^{-3} (2.5 ppb) (Graaf et al., 2018;Van Damme et al., 2014a). Similarly, we also compared the surface NH_3 concentrations (at the first layer) simulated by GEOS-Chem with the monitoring results (R^2=0.54 and RMSE=2.14 μg N m^{-3} in **Fig. 3**). In general, IASI-derived surface NH_3 concentrations had better consistency with the ground-based measurements than those from GEOS-Chem over China, the US and Europe. The relatively low accuracy from GEOS-Chem was likely due to the coarse model resolutions as well as the poor spatiotemporal representations of NH_3 emissions, as suggested by a previous study (Zhang et al., 2018).

A known limitation of IASI NH_3 retrievals is lack of the vertical profile information.

A previous study (Van Damme et al., 2014a) used fixed profiles on the land to convert the IASI NH_3 columns to surface NH_3 concentrations. Using the fixed profiles can cause large uncertainties for estimating surface NH_3 concentrations. In this work, we utilized the advantages of CTMs and considered the spatial variability of the vertical profiles, and proves that IASI NH_3 columns are powerful to predict the surface NH_3 concentrations combining the vertical profiles simulated by Gaussian function.

Through the Gaussian simulation of NH_3 vertical profiles, we are able to evaluate the sensitive regions of surface NH_3 concentrations with respect to different heights. **Fig. S5** shows the spatial distribution of the difference of NH_3 concentrations between 40m and 60m (about the middle height of the first layer in GEOS-Chem). In general, in strong NH_3 emission regions, there is a relatively large difference in surface NH_3 concentrations such as, for instance, in eastern China and northwestern India (can be up to 3 μg N m^{-3}); subsequently, a middle difference (2-3 μg N m^{-3}) occurs in eastern and middle China, northern India and northern Italy. Except above mentioned regions, the difference of NH_3 concentrations between 40m and 60m is generally lower 0.5 μg N m^{-3}.

Spatial distributions of satellite-derived surface NH_3 concentrations

Fig. 4 shows the spatial distributions of surface NH_3 concentrations in China, US and Europe in 2014. The overall mean surface NH_3 concentrations over China were 2.38 μg N m^{-3}, with the range of 0.22-13.11 μg N m^{-3}. We found large areas in eastern China (109-122^o E, 28-41^o N), Sichuan Basin, Hubei (including Wuhan, Xiangyang and Yichang), Shaanxi (including Xi'an, Baoji, Hanzhong, Weinan), Gansu (Lanzhou and its surrounding areas), Shanxi (including Yuncheng and Changzhi) and northwestern Xinjiang with surface NH_3 concentrations greater than 8 μg N m^{-3} y^{-1}, which were in agreement with the spatial distributions of the croplands in China (**Fig. S6**). It is not surprising that high surface NH_3 concentrations occurred in eastern China and Sichuan Basin because the major Chinese croplands are distributed there, as the major source of NH_3 emissions with frequent N fertilizer applications. In addition, N manure is another major source of NH_3 emissions in China, and the

372 percentage of N manure to NH_3 emissions exceeds 50% (Kang et al., 2016). Overall,
373 there was a significant linear correlation between surface NH_3 concentration and N
374 fertilization plus N manure in China (R^2=0.69, p=0.000 in **Fig. 5**). The hotspots also
375 occurred in northwestern Xinjiang surrounding the cropland areas, which may be
376 related to the dry climate that can maintain NH_3 in the gaseous state for a longer time,
377 providing climate conditions for the long distance transmission of NH_3. Recent
378 national measurement work (Pan et al., 2018) also revealed high surface NH_3
379 concentrations in northwestern Xinjiang, confirming the rationality of the
380 IASI-derived estimates.
381 In the US, the overall mean surface NH_3 concentrations were 1.52 μg N m^{-3} y^{-1}, with
382 the range of 0.14-10.60 μg N m^{-3}. The surface NH_3 hotspots were generally
383 distributed in the croplands in the central and eastern US (such as Ohio, Illinois, South
384 Dakota, Nebraska, Kansas, Minnesota and North Dakota), as well as in some small
385 areas in western coastal regions (such as California and Washington). In particular, the
386 San Joaquin Valley (SJV) in California (an agricultural land) had the highest surface
387 NH_3 concentrations greater than 4 μg N m^{-3}. The NH_3 source in SJV was from
388 livestock and mineral N fertilizer, which accounted for 74% and 16% of total NH_3
389 emissions, respectively (Simon et al., 2008). Except the SJV in California, the annual
390 surface NH_3 concentrations in the croplands were mostly within the range of 1-3 μg N
391 m^{-3}, which were much lower than those in eastern China (mostly within the range of
392 4-10 μg N m^{-3}). Compared with the spatial distribution of N fertilization plus N
393 manure, the hotspots of surface NH_3 concentration can basically reflect the
394 distribution of high N fertilization (R^2=0.37, p=0.000 in **Fig 4 and Fig. 5**).
395 In Europe, the overall mean surface NH_3 concentrations were 1.8 μg N m^{-3}, with the
396 range of 0.04-9.49 μg N m^{-3}. High surface NH_3 concentrations were distributed
397 widespread in the croplands, especially in the western regions with values greater than
398 4 μg N m^{-3}, such as Northern Italy (Milan and its surrounding areas), Switzerland,
399 central and southern Germany, Eastern France (Paris and its surrounding areas) and
400 Poland. According to Emissions Database for Global Atmospheric Research
401 (EDGAR), N manure and N fertilization accounts for 53% and 43% of the NH_3

emissions in western Europe. Overall, there was also a significant linear correlation between surface NH_3 concentration and N fertilization plus N manure (R^2=0.39, p=0.000) in Europe, reflecting the importance of N fertilization on surface NH_3 concentration.

NH_3 is the most abundant alkaline gas in the atmosphere, and has implications to neutralize acidic species (such as H_2SO_4 and HNO_3) to form ammonium salts (such as $(NH_4)_2SO_4$ and NH_4NO_3). Ammonium salts are the important inorganic N components in PM2.5, which can reduce regional visibility and contribute to human disease burden (Van et al., 2015;Yu et al., 2007). Comparing surface NH_3 concentrations with PM2.5 can benefit the understanding of the sources and the mixture of air pollution. The spatial distribution of satellite-derived $PM_{2.5}$ (dust and sea-salt removed) in 2014 (**Fig. S7**) gained from a previous study (Van et al., 2016) was compared with the satellite-derived surface NH_3 concentrations in 2014. On the other hand, NO_2 is also an important precursor of nitrate salts in $PM_{2.5}$. We also included the satellite-derived surface NO_2 concentrations (**Fig. S7**) from a previous study (Geddes et al., 2016) to compare with surface NH_3 and $PM_{2.5}$ concentrations.

The hotspots of surface NH_3 concentrations were highly linked with the hotspots of $PM_{2.5}$. The most severe pollution occurred in the eastern China with annual average $PM_{2.5}$ exceeding 50 μg m^{-3} (much higher than 35 μg m^{-3} as the level 2 annual $PM_{2.5}$ standard set by World Health Organization Air Quality Interim Target-1), and annual average surface NH_3 and NO_2 concentrations greater than 8 μg N m^{-3} and 4 μg N m^{-3}, respectively. A previous study (Xu et al., 2017) reported that the secondary inorganic aerosols of NH_4^+ and NO_3^- can account for 65% of $PM_{2.5}$ based on the measurements in three sites in Beijing. NH_3 and NO_2 are the most important precursors of nitrate salts and ammonium salts, and certainly contribute to the severe pollution in the eastern China. The second severe pollution occurred in the northern India with annual average $PM_{2.5}$ and surface NH_3 concentrations exceeding 40 μg m^{-3} and 4 μg N m^{-3} respectively (surface NO_2 concentrations less than 1 μg N m^{-3}). The major source of NH_3 in northern India was from agricultural activities and livestock waste management (Warner et al., 2016). The hotspots of surface NH_3 concentrations in the

central and eastern US were highly related to the hotspots of $PM_{2.5}$. The annual average $PM_{2.5}$ is less than 10 μg m^{-3} (the first level set by World Health Organization) in the most areas of the US, and only small areas had $PM_{2.5}$ greater than 10 μg m^{-3}. Similarly, in western Europe, the hotspots of high surface NH_3 and NO_2 concentrations (greater than 3 μg N m^{-3}) were consistent with the hotspots of $PM_{2.5}$ (greater than 20 μg m^{-3}).

Seasonal variations of satellite-derived surface NH_3 concentrations

To investigate the seasonal variations of surface NH_3 concentrations, we took the monthly surface NH_3 concentrations in 2014 as a case study (**Fig. 6)**, and analyzed the seasonal surface NH_3 concentrations in hotspot regions including East China (ECH), Sichuan and Chongqing (SCH), Guangdong (GD), Northeast India (NEI), East US (EUS) and West Europe (WEU) (**Fig. 7**).

Seasonal mean IASI-derived surface NH_3 concentrations vary by more than 2 orders of magnitude in hotspot regions, such as the eastern China and eastern US. In China, high surface NH_3 concentrations occurred in spring (March, April and May) and summer (June, July and August) in East China (ECH), Sichuan and Chongqing (SCH), Guangdong (GD). This may be due to two major reasons. First, the timing of the mineral N fertilizer or manure application occurred in summer or spring in the croplands (Paulot et al., 2014). A previous study (Huang et al., 2012) also suggested a summer peak in NH_3 emissions in China, which was consistent with the summer peak in surface NH_3 concentrations. Second, the temperature in warm months is highest in one year, which favors the volatilization of ammonium ($NH_4^+ + OH^- \rightarrow NH_3 + H_2O$). Notably, there is a difference in the seasonal variations of surface NH_3 concentrations between ECH (peaking in June and July) and GD (peaking in March), which was likely related to different crop planting, N fertilization time as well as meteorological factors (Van Damme et al., 2015;Shen et al., 2009;Van Damme et al., 2014a). In the eastern US (EUS), high surface NH_3 concentrations appeared in warm months (from March to August, **Fig. 7**) with the maximum in May due to higher temperature and emissions in vast croplands, where the agricultural mineral N fertilizers dominate the

NH_3 emissions. A previous study also implied a spring peak in NH_3 emissions in the eastern US (Gilliland et al., 2006). Since the spatial patterns of high surface NH_3 concentrations are highly linked with the spatial distributions of croplands, seasonal surface NH_3 concentrations mainly reflects the timing of N fertilizers in the croplands. In western Europe, surface NH_3 concentrations is low in January and February, rising in March and reaching its maximum, keeping high from March to June, then declining from June to December (**Fig. 7**). High NH_3 concentrations appeared from March to June, mainly affected by higher temperature and frequent N fertilization (Van Damme et al., 2014b;Paulot et al., 2014;Van Damme et al., 2015;Whitburn et al., 2015).

To identify the major regions of biomass burning that may affect the spatial distribution of surface NH_3 concentrations, we used the fire products from the moderate resolution imaging spectroradiometer (MODIS) on board the NASA Aqua and Terra. The MODIS climate modeling grid (CMG) global monthly fire location product (level 2, collection 6) developed by the University of Maryland included geographic location of fire, raw count of fire pixels and mean fire radiative power (Giglio et al., 2015). We used the Aqua and Terra CMG fire products on a monthly scale at a spatial resolution of $0.5\,^{\circ}\text{latitude} \times 0.5\,^{\circ}\text{longitude}$ in 2014, and the fire pixel counts were used to identify the hotspot regions of biomass burning. In the major hotspots with frequent fires (mostly in the southern hemisphere), the biomass burning controlled the seasonal surface NH_3 concentrations (**Fig. S8 and Fig. S9**), such as, for instance, Africa north of equator, Africa south of equator and central South America. Apart from the large areas with frequent fires in the southern hemisphere, we also demonstrated the relationship of biomass burning and surface NH_3 concentrations in China, US and Europe, and selected six typical regions in China (CH1 and CH2), US (US1 and US2) and Europe (EU1 and EU2) (**Fig. 8**) to analyze the monthly variations of fire counts and surface NH_3 concentrations.

In China, the first region (CH1) covers the major cropland areas in northern China including Shandong, Henan and and northern Jiangsu Provinces. The fires counts were mainly from the crop straw burning, which contributes large to surface NH_3 concentrations. Both surface NH_3 concentrations and fire counts were found in June

likely related to the crop straw burning in this agricultural regions. Notably, despite a decline in fire counts in July, the surface NH_3 concentrations in July did not decrease, probably due to mineral N fertilization for new planted crops (CH1 is typical for spring and summer corn rotations) as well as the high temperature favoring NH_3 volatilization in July. The second region (CH2) is typical for the rice cultivation area in the southern China, where the rice was normally planted in June or July with frequent mineral N fertilization. Thus, the highest surface NH_3 concentrations occurred in June and July. This region is also typical for the winter wheat and summer rice rotations, and the wheat is normally harvested from May to July, which can lead to frequent fire counts there. Despite the more frequent fires in the second region than the first region, the surface NH_3 concentrations in CH2 were much lower than those in CH1. This may be due to the wetter climate and more frequent precipitation events in CH2 than in CH1, resulting in higher scavenging of surface NH_3 concentrations into water.

US1 is a region typical for forest land in the US, and the fire counts are certainly from the forest fires or anthropogenic biomass burning. The monthly variations of surface NH_3 concentrations were consistent with the monthly variations of MODIS fire counts, which peaked in August with high temperature. Instead, US2 is a region typical for mixed agricultural and forest lands, which can be influenced by both potential mineral N fertilization and anthropogenic biomass burning or forest fires. It is clear to see that there is a peak in surface NH_3 concentrations in October resulting from the biomass burning because of the same peak in fire counts in October. However, there is also an apparent peak in surface NH_3 concentrations in May, which may result from the mineral N fertilization in this region. In Europe, the selected two regions of EU1 and EU2 are mainly covered by crops, vegetables as well as forests. For EU2, the monthly variations of surface NH_3 concentrations were consistent with the monthly variations of MODIS fire counts, which peaked in August with high temperature, implying that the biomass burning may control the seasonal surface NH_3 concentrations. For EU1, there were two peaks of surface NH_3 concentrations including April and August. The August peak can be related to the biomass burning because of the high fire counts,

while the April peak may be related to the agricultural fertilizations for the spring crops.

Trends in surface NH_3 concentrations in China, the US and Europe

Time series of nine years' (2008-2016) IASI-derived surface NH_3 concentrations have been fitted using the linear regression method (Geddes et al., 2016;Richter et al., 2005) for all grids on the land. The annual trend (the slope of the linear regression model) is shown in **Fig. 9**. A significant increase rate of surface NH_3 concentrations (>0.2 μg N m^{-3} y^{-1}) appeared in eastern China, and a middle positive trend (0.1-0.2 μg N m^{-3} y^{-1}) occurred in northern Xinjiang, corresponding to its frequent agricultural activities for fertilized crops and dry climate (Warner et al., 2017;Liu et al., 2017b;Xu et al., 2015;Huang et al., 2012). The large increase in eastern China was consistent with the results revealed by AIRS NH_3 data (Warner et al., 2017). The increase of surface NH_3 concentrations in eastern China was consistent with the trend of NH_3 emission estimates by a recent study (Zhang et al., 2017b). China's NH_3 emissions increased significantly from 2008 to 2015, with an increase rate of 1.9% y^{-1}, which was mainly driven by eastern China (Zhang et al., 2017b). Approximately 85% of the inter-annual variations was due to the changes of human activities, and the remaining 15% resulted from air temperature changes. Agricultural activities is the main drive of NH_3 emission increase, of which 43.1% and 36.4% were contributed by livestock manure and fertilizer application (Zhang et al., 2017b). In addition, the increase in surface NH_3 concentrations in eastern China may be also linked with the decreased NH_3 removal due to the decline in acidic gases (NO_2 and SO_2) (Liu et al., 2017a;Xia et al., 2016). NH_3 can react with nitric acid and sulfuric acid to form ammonia sulfate and ammonia nitrate aerosols. The reduction of acidic gases leads to the reduction of NH_3 conversion to ammonia salts in the atmosphere, which may lead to the increase of NH_3 in the atmosphere (Liu et al., 2017a;Li et al., 2017b). China's SO_2 emissions decreased by about 60% in 2008-2016, which led to a 50% decrease in surface SO_2 concentrations simulated by WRF model, and then resulted in a 30% increase in surface NH_3 concentrations (Liu et al., 2018).

In the US, the NH_3 increase was found in agricultural regions in middle and eastern regions with an annual increase rate of lower than 0.10 μg N m^{-3} y^{-1}, which was consistent with the results of AIRS NH_3 data for a longer time period (2003-2016) (Warner et al., 2017), while we concerned the timespan of 2008-2016 from IASI retrievals. Based on the simulation data of CMAQ model, it is also found that NH_3 increased significantly in the eastern US from 1990 to 2010, which is inconsistent with the significant downward trend of NO_x emissions (Zhang et al., 2018). This inconsistency between NH_3 and NO_x trends in the US was mainly due to different emission control policies. Over the past two decades, due to the implementation of effective regulations and emission reduction measures for NO_x, the NO_x emission in the US decreased by nearly 41% between 1990 and 2010 (Hand et al., 2014). However, this NH_3 increase in eastern US is likely due to the lack of NH_3 emission control policy as well as the decreased NH_3 removal due to the decline in acidic gases (NO_2 and SO_2) (Warner et al., 2017;Li et al., 2016). As NH_3 is an uncontrolled gas in the US, NH_3 emissions have continuously increased since 1990, and by 2003 NH_3 emissions had begun to dominate the inorganic N emissions (NO_x plus NH_3) (Zhang et al., 2018). For the western Europe, the trend was close to 0 in most regions although we can observe the NH_3 increase in many points with small positive trend of lower than 0.1 μg N m^{-3} y^{-1}. Compared with the trend of surface NH_3 concentrations in China and the US, the change of surface NH_3 concentrations in western Europe is more stable, which may be related to the mature NH_3 reduction policies and measures in Europe. Since 1990, Europe has implemented a series of agricultural NH_3 emission reduction measures, and NH_3 emissions decreased by about 29% between 1990 and 2009 (Tørseth et al., 2012b). For example, due to serious N eutrophication, the Netherlands has taken measures to reduce NH_3 emissions by nearly two times in the past 20 years, while maintaining a high level of food production (Dentener et al., 2006). The N fertilizer use in Europe has decreased widespread according to the data from the World Bank (http://data.worldbank.org/indicator/AG.CON.FERT.ZS) with an annual decrease of -8.84~-17.7 kg ha^{-1} y^{-1} in fertilizer use in Europe (Warner et al., 2017).

Conclusions

The IASI-derived global surface NH_3 concentrations during 2008-2016 were inferred based on IASI NH_3 column measurements as well as NH_3 vertical profiles from the GEOS-Chem in this study. Global NH_3 vertical profiles on the land from the GEOS-Chem can be well modelled by the Gaussian function between 60 °N and 55 °S with R^2 higher than 0.90. The IASI-derived surface NH_3 concentrations were compared to the in situ measurements over China, the US and Europe. One of the major findings is that a relatively high predictive power for annual surface NH_3 concentrations was achieved through converting IASI NH_3 columns using modelled NH_3 vertical profiles, and the validation with the ground-based measurements shows that IASI-derived surface NH_3 concentrations had higher accuracy in China than the US and Europe. High surface NH_3 concentrations were found in the croplands in China, US and Europe, and surface NH_3 concentrations in the croplands in China were approximately double than those in the US and Europe. Seasonal mean IASI-derived surface NH_3 concentrations vary by more than 2 orders of magnitude in hotspot regions, such as the eastern China and eastern US. The linear trend analysis shows that a significant positive increase rate of above 0.2 μg N m^{-3} y^{-1} appeared in the eastern China during 2008-2016, and a middle increase trend (0.1-0.2 μg N m^{-3} y^{-1}) occurred in northern Xinjiang Province. In the US, the NH_3 increase was found in agricultural regions in middle and eastern regions with an annual increase rate of lower than 0.10 μg N m^{-3} y^{-1}.

Author contributions

LL and XZ designed the research; WX and XL's group conducted the field work in China; LL prepared IASI NH_3 products; LL and AW conducted model simulations; LL, WX, LZ, XW and ZW performed the data analysis and prepared the figures; LL, AW and XZ wrote the paper, and all coauthors contribute to the revision.

Acknowledgements

We acknowledge the free use of IASI NH_3 data from the Atmospheric Spectroscopy Group at Universit élibre de Bruxelles (ULB). We thank Dr. Jeffrrey A. Geddes for the help of using the GEOS-Chem in this work. This study is supported by the National Natural Science Foundation of China (No. 41471343, 41425007 and 41101315) and Doctoral Research Innovation Fund (2016CL07) as well as the Chinese National Programs on Heavy Air Pollution Mechanisms and Enhanced Prevention Measures (Project No. 8 in the 2nd Special Program).

Data availability

The IASI NH_3 satellite datasets are available at: http://iasi.aeris-data.fr/NH3. The ground-based NH_3 mesurements in Chinese Nationwide Nitrogen Deposition Monitoring Network (NNDMN) can be requested from Prof. Xuejun Liu in China Agricutural University. The ground-based NH_3 measurements from the AMoN-US can be downloaded from the website: http://nadp.sws.uiuc.edu/AMoN/. The ground-based NH_3 measurements from the EMEP network can be gained from https://www.nilu.no/projects/ccc/emepdata.html. The IASI-derived surface NH_3 used in this study are available from the corresponding author upon request.

Notes

The authors declare that they have no conflict of interest.

Reference

Amos, H. M., Jacob, D. J., Holmes, C. D., Fisher, J. A., Wang, Q., Yantosca, R. M., Corbitt, E. S., Galarneau, E., Rutter, A. P., and Gustin, M. S.: Gas-particle partitioning of atmospheric Hg(II) and its effect on global mercury deposition, Atmospheric Chemistry & Physics, 11, 29441-29477, 2012.

Basto, S., Thompson, K., Phoenix, G., Sloan, V., Leake, J., and Rees, M.: Long-term nitrogen deposition depletes grassland seed banks, Nature Communication, 6, 1-6,

10.1038/ncomms7185, 2015.

Bobrutzki, K. V., Braban, C. F., Famulari, D., Jones, S. K., Blackall, T., Smith, T. E. L., Blom, M., Coe, H., Gallagher, M., and Ghalaieny, M.: Field inter-comparison of eleven atmospheric ammonia measurement techniques, Atmospheric Measurement Techniques,3,1(2010-01-27), 2, 91-112, 2010.

Crippa, M., Guizzardi, D., Muntean, M., Schaaf, E., Dentener, F., van Aardenne, J. A., Monni, S., Doering, U., Olivier, J. G. J., Pagliari, V., and Janssens-Maenhout, G.: Gridded emissions of air pollutants for the period 1970–2012 within EDGAR v4.3.2, Earth Syst. Sci. Data, 10, 1987-2013, 10.5194/essd-10-1987-2018, 2018.

Dammers, E., Palm, M., Van Damme, M., Vigouroux, C., Smale, D., Conway, S., Toon, G. C., Jones, N., Nussbaumer, E., Warneke, T., Petri, C., Clarisse, L., Clerbaux, C., Hermans, C., Lutsch, E., Strong, K., Hannigan, J. W., Nakajima, H., Morino, I., Herrera, B., Stremme, W., Grutter, M., Schaap, M., Wichink Kruit, R. J., Notholt, J., Coheur, P. F., and Erisman, J. W.: An evaluation of IASI-NH_3 with ground-based Fourier transform infrared spectroscopy measurements, Atmospheric Chemistry and Physics, 16, 10351-10368, 10.5194/acp-16-10351-2016, 2016.

Dentener, F., Drevet, J., Lamarque, J., Bey, I., Eickhout, B., Fiore, A., Hauglustaine, D., Horowitz, L., Krol, M., and Kulshrestha, U.: Nitrogen and sulfur deposition on regional and global scales: a multimodel evaluation, Global Biogeochemical Cycles, 20, 2006.

Eerden, L. J. M. V. D.: Toxicity of ammonia to plants, Agriculture & Environment, 7, 223-235, 1982.

Fountoukis, C., and Nenes, A.: ISORROPIA II: a computationally efficient thermodynamic equilibrium model for aerosols, Atmospheric Chemistry and Physics, 7, 4639-4659, 2007.

Geddes, J. A., Martin, R. V., Boys, B. L., and van Donkelaar, A.: Long-term trends worldwide in ambient NO_2 concentrations inferred from satellite observations, Environmental Health Perspectives, 124, 281, 2016.

Geng, G., Zhang, Q., Martin, R. V., Donkelaar, A. V., Huo, H., Che, H., Lin, J., and He, K.: Estimating long-term PM 2.5 concentrations in China using satellite-based

662 aerosol optical depth and a chemical transport model, Remote Sensing of
663 Environment, 166, 262-270, 2015.
664 Giglio, L., Randerson, J. T., and van der Werf, G. R.: Analysis of daily, monthly, and
665 annual burned area using the fourth-generation global fire emissions database
666 (GFED4), Journal of Geophysical Research: Biogeosciences, 118, 317-328,
667 10.1002/jgrg.20042, 2013.
668 Giglio, L., Csiszar, I., and Justice, C. O.: Global distribution and seasonality of active
669 fires as observed with the Terra and Aqua Moderate Resolution Imaging
670 Spectroradiometer (MODIS) sensors, Journal of Geophysical Research
671 Biogeosciences, 111, 17-23, 2015.
672 Gilliland, A. B., Wyat Appel, K., Pinder, R. W., and Dennis, R. L.: Seasonal NH_3
673 emissions for the continental united states: Inverse model estimation and evaluation,
674 Atmospheric Environment, 40, 4986-4998,
675 https://doi.org/10.1016/j.atmosenv.2005.12.066, 2006.
676 Graaf, S. C. v. d., Dammers, E., Schaap, M., and Erisman, J. W.: How are NH_3 dry
677 deposition estimates affected by combining the LOTOS-EUROS model with
678 IASI-NH3 satellite observations?, Atmospheric Chemistry and Physics, 18,
679 13173-13196, https://doi.org/10.5194/acp-2018-133, 2018.
680 Hand, J. L., Schichtel, B. A., Malm, W. C., Copeland, S., Molenar, J. V., Frank, N.,
681 and Pitchford, M.: Widespread reductions in haze across the United States from the
682 early 1990s through 2011, Atmospheric Environment, 94, 671-679, 2014.
683 Huang, X., Song, Y., Li, M., Li, J., Huo, Q., Cai, X., Zhu, T., Hu, M., and Zhang, H.:
684 A high resolution ammonia emission inventory in China, Global Biogeochemical
685 Cycles, 26, 1-14, 2012.
686 Janssens-Maenhout, G., Crippa, M., Guizzardi, D., Dentener, F., Muntean, M., Pouliot,
687 G., Keating, T., Zhang, Q., Kurokawa, J., Wankmüller, R., Denier van der Gon, H.,
688 Kuenen, J. J. P., Klimont, Z., Frost, G., Darras, S., Koffi, B., and Li, M.: HTAP_v2.2:
689 a mosaic of regional and global emission grid maps for 2008 and 2010 to study
690 hemispheric transport of air pollution, Atmos. Chem. Phys., 15, 11411-11432,
691 10.5194/acp-15-11411-2015, 2015.

692 Kang, Y., Liu, M., Song, Y., Huang, X., Yao, H., Cai, X., Zhang, H., Kang, L., Liu, X.,
693 Yan, X., He, H., Zhang, Q., Shao, M., and Zhu, T.: High-resolution ammonia
694 emissions inventories in China from 1980 to 2012, Atmospheric Chemistry and
695 Physics, 16, 2043-2058, 10.5194/acp-16-2043-2016, 2016.
696 Kharol, S. K., Shephard, M. W., McLinden, C. A., Zhang, L., Sioris, C. E., O'Brien, J.
697 M., Vet, R., Cady-Pereira, K. E., Hare, E., Siemons, J., and Krotkov, N. A.: Dry
698 Deposition of Reactive Nitrogen From Satellite Observations of Ammonia and
699 Nitrogen Dioxide Over North America, Geophysical Research Letters, 45, 1157-1166,
700 10.1002/2017GL075832, 2018.
701 Kim, T. W., Lee, K., Duce, R., and Liss, P.: Impact of atmospheric nitrogen deposition
702 on phytoplankton productivity in the South China Sea, Geophysical Research Letters,
703 41, 3156–3162, 2014.
704 Lamarque, J. F., Kiehl, J., Brasseur, G., Butler, T., Cameron‐Smith, P., Collins, W.,
705 Collins, W., Granier, C., Hauglustaine, D., and Hess, P.: Assessing future nitrogen
706 deposition and carbon cycle feedback using a multimodel approach: Analysis of
707 nitrogen deposition, Journal of Geophysical Research: Atmospheres (1984–2012), 110,
708 2005.
709 Lamsal, L. N., Martin, R. V., van Donkelaar, A., Steinbacher, M., Celarier, E. A.,
710 Bucsela, E., Dunlea, E. J., and Pinto, J. P.: Ground-level nitrogen dioxide
711 concentrations inferred from the satellite-borne Ozone Monitoring Instrument, Journal
712 of Geophysical Research: Atmospheres, 113, 1-15, 10.1029/2007JD009235, 2008.
713 Lamsal, L. N., Martin, R. V., Parrish, D. D., and Krotkov, N. A.: Scaling relationship
714 for NO_2 pollution and urban population size: a satellite perspective, Environmental
715 Science & Technology, 47, 7855-7861, 2013.
716 Larssen, T., Duan, L., and Mulder, J.: Deposition and leaching of sulfur, nitrogen and
717 calcium in four forested catchments in China: implications for acidification,
718 Environmental science & technology, 45, 1192-1198, 2011.
719 Lenhart, L., and Friedrich, R.: European emission data with high temporal and spatial
720 resolution, Water Air & Soil Pollution, 85, 1897-1902, 1995.
721 Levine, J. S., Augustsson, T. R., and Hoell, J. M.: The vertical distribution of

722 tropospheric ammonia, Geophysical Research Letters, 7, 317-320,
723 10.1029/GL007i005p00317, 1980.
724 Li, M., Zhang, Q., Kurokawa, J., Woo, J. H., He, K., Lu, Z., Ohara, T., Song, Y.,
725 Streets, D. G., and Carmichael, G. R.: MIX: a mosaic Asian anthropogenic emission
726 inventory under the international collaboration framework of the MICS-Asia and
727 HTAP, Atmospheric Chemistry & Physics, 17, 34813-34869, 2017a.
728 Li, Y., Schwandner, F. M., Sewell, H. J., Zivkovich, A., Tigges, M., Raja, S., Holcomb,
729 S., Molenar, J. V., Sherman, L., and Archuleta, C.: Observations of ammonia, nitric
730 acid, and fine particles in a rural gas production region, Atmospheric Environment, 83,
731 80-89, 2014.
732 Li, Y., Schichtel, B. A., Walker, J. T., Schwede, D. B., Chen, X., Lehmann, C. M.,
733 Puchalski, M. A., Gay, D. A., and Collett, J. L.: Increasing importance of deposition of
734 reduced nitrogen in the United States, Proceedings of the National Academy of
735 Sciences, 113, 5874-5879, 2016.
736 Li, Y., Thompson, T. M., Damme, M. V., Chen, X., Benedict, K. B., Shao, Y., Day, D.,
737 Boris, A., Sullivan, A. P., and Ham, J.: Temporal and Spatial Variability of Ammonia
738 in Urban and Agricultural Regions of Northern Colorado, United States, Atmospheric
739 Chemistry & Physics, 17, 1-50, 2017b.
740 Lin, J. T., Martin, R. V., Boersma, K. F., Sneep, M., Stammes, P., Spurr, R., Wang, P.,
741 Van Roozendael, M., Clémer, K., and Irie, H.: Retrieving tropospheric nitrogen
742 dioxide from the Ozone Monitoring Instrument: effects of aerosols, surface
743 reflectance anisotropy, and vertical profile of nitrogen dioxide, Atmospheric
744 Chemistry and Physics, 14, 1441-1461, 10.5194/acp-14-1441-2014, 2014.
745 Liu, H., Jacob, D. J., Bey, I., and Yantosca, R. M.: Constraints from 210Pb and 7Be on
746 wet deposition and transport in a global three-dimensional chemical tracer model
747 driven by assimilated meteorological fields, Journal of Geophysical Research:
748 Atmospheres, 106, 12109-12128, 10.1029/2000JD900839, 2001.
749 Liu, L., Zhang, X., Xu, W., Liu, X., Li, Y., Lu, X., Zhang, Y., and Zhang, W.:
750 Temporal characteristics of atmospheric ammonia and nitrogen dioxide over China
751 based on emission data, satellite observations and atmospheric transport modeling

since 1980, Atmospheric Chemistry & Physics, 17, 1-32, 2017a.

Liu, L., Zhang, X., Xu, W., Liu, X., Lu, X., Wang, S., Zhang, W., and Zhao, L.: Ground Ammonia Concentrations over China Derived from Satellite and Atmospheric Transport Modeling, Remote Sensing, 9, 467, 2017b.

Liu, L., Zhang, X., Zhang, Y., Xu, W., Liu, X., Zhang, X., Feng, J., Chen, X., Zhang, Y., Lu, X., Wang, S., Zhang, W., and Zhao, L.: Dry Particulate Nitrate Deposition in China, Environmental Science & Technology, 51, 5572-5581, 10.1021/acs.est.7b00898, 2017c.

Liu, M., Huang, X., Song, Y., Xu, T., Wang, S., Wu, Z., Hu, M., Zhang, L., Zhang, Q., Pan, Y., Liu, X., and Zhu, T.: Rapid SO_2 emission reductions significantly increase tropospheric ammonia concentrations over the North China Plain, Atmospheric Chemistry and Physics, 18, 17933-17943, 10.5194/acp-18-17933-2018, 2018.

Mao, J., Paulot, F., Jacob, D. J., Cohen, R. C., Crounse, J. D., Wennberg, P. O., Keller, C. A., Hudman, R. C., Barkley, M. P., and Horowitz, L. W.: Ozone and organic nitrates over the eastern United States: Sensitivity to isoprene chemistry, Journal of Geophysical Research Atmospheres, 118, 11-11,268, 2013.

Nowlan, C., Martin, R., Philip, S., Lamsal, L., Krotkov, N., Marais, E., Wang, S., and Zhang, Q.: Global dry deposition of nitrogen dioxide and sulfur dioxide inferred from space-based measurements, Global Biogeochemical Cycles, 28, 1025-1043, 2014.

Pan, Y., Tian, S., Zhao, Y., Zhang, L., Zhu, X., Gao, J., Huang, W., Zhou, Y., Song, Y., and Zhang, Q.: Identifying ammonia hotspots in China using a national observation network, Environmental Science & Technology, 2018.

Paulot, F., Jacob, D. J., Pinder, R. W., Bash, J. O., Travis, K., and Henze, D. K.: Ammonia emissions in the United States, European Union, and China derived by high-resolution inversion of ammonium wet deposition data: Interpretation with a new agricultural emissions inventory (MASAGE_NH_3), Journal of Geophysical Research: Atmospheres, 119, 4343-4364, 10.1002/2013JD021130, 2014.

Potter, P., Ramankutty, N., Bennett, E. M., and Donner, S. D.: Characterizing the Spatial Patterns of Global Fertilizer Application and Manure Production, Earth Interactions, 14, 1-22, 10.1175/2009EI288.1, 2010.

782 Preston, K. E., Jones, R. L., and Roscoe, H. K.: Retrieval of NO_2 vertical profiles
783 from ground-based UV-visible measurements: Method and validation, Journal of
784 Geophysical Research: Atmospheres, 102, 19089-19097, doi:10.1029/97JD00603,
785 1997.
786 Puchalski, M. A., Sather, M. E., Walker, J. T., Lehmann, C. M. B., Gay, D. A.,
787 Johnson, M., and Robarge, W. P.: Passive ammonia monitoring in the United States:
788 comparing three different sampling devices, Journal of Environmental Monitoring, 13,
789 3156, 2011.
790 Pye, H. O. T., Liao, H., Wu, S., Mickley, L. J., Jacob, D. J., Henze, D. K., and
791 Seinfeld, J. H.: Effect of changes in climate and emissions on future
792 sulfate-nitrate-ammonium aerosol levels in the United States, Journal of Geophysical
793 Research: Atmospheres, 114, doi:10.1029/2008JD010701, 2009.
794 Reay, D. S., Dentener, F., Smith, P., Grace, J., and Feely, R. A.: Global nitrogen
795 deposition and carbon sinks, Nature Geoscience, 1, 430-437, 2008.
796 Richter, A., Burrows, J. P., Nüß, H., Granier, C., and Niemeier, U.: Increase in
797 tropospheric nitrogen dioxide over China observed from space, Nature, 437, 129-132,
798 2005.
799 Rozanov, A., Bovensmann, H., Bracher, A., Hrechanyy, S., Rozanov, V., Sinnhuber,
800 M., Stroh, F., and Burrows, J. P.: NO2 and BrO vertical profile retrieval from
801 SCIAMACHY limb measurements: Sensitivity studies, Advances in Space Research,
802 36, 846-854, https://doi.org/10.1016/j.asr.2005.03.013, 2005.
803 Schaap, M., van Loon, M., ten Brink, H. M., Dentener, F. J., and Builtjes, P. J. H.:
804 Secondary inorganic aerosol simulations for Europe with special attention to nitrate,
805 Atmos. Chem. Phys., 4, 857-874, 10.5194/acp-4-857-2004, 2004.
806 Schiferl, L. D., Heald, C. L., Nowak, J. B., Holloway, J. S., Neuman, J. A., Bahreini,
807 R., Pollack, I. B., Ryerson, T. B., Wiedinmyer, C., and Murphy, J. G.: An investigation
808 of ammonia and inorganic particulate matter in California during the CalNex
809 campaign, Journal of Geophysical Research: Atmospheres, 119, 1883-1902, 2014.
810 Schiferl, L. D., Heald, C. L., Van Damme, M., Pierrefrancois, C., and Clerbaux, C.:
811 Interannual Variability of Ammonia Concentrations over the United States: Sources

812 and Implications for Inorganic Particulate Matter, Atmospheric Chemistry & Physics,
813 1-42, 2015.
814 Shen, J. L., Tang, A. H., Liu, X. J., Fangmeier, A., Goulding, K. T. W., and Zhang, F.
815 S.: High concentrations and dry deposition of reactive nitrogen species at two sites in
816 the North China Plain, Environmental Pollution, 157, 3106-3113,
817 http://dx.doi.org/10.1016/j.envpol.2009.05.016, 2009.
818 Shephard, M., and Cady-Pereira, K.: Cross-track Infrared Sounder (CrIS) satellite
819 observations of tropospheric ammonia, Atmospheric Measurement Techniques, 8,
820 1323-1336, 2015.
821 Shephard, M. W., Cady-Pereira, K. E., Luo, M., Henze, D. K., Pinder, R. W., Walker, J.
822 T., Rinsland, C. P., Bash, J. O., Zhu, L., Payne, V. H., and Clarisse, L.: TES ammonia
823 retrieval strategy and global observations of the spatial and seasonal variability of
824 ammonia, Atmos. Chem. Phys., 11, 10743-10763, 10.5194/acp-11-10743-2011, 2011.
825 Sheppard, L. J., Leith, I. D., Crossley, A., Dijk, N. V., Fowler, D., Sutton, M. A., and
826 Woods, C.: Stress responses of Calluna vulgaris to reduced and oxidised N applied
827 under 'real world conditions', Environmental Pollution, 154, 404-413, 2008.
828 Simon, H., Allen, D. T., and Wittig, A. E.: Fine particulate matter emissions
829 inventories: comparisons of emissions estimates with observations from recent field
830 programs, Journal of the Air & Waste Management Association, 58, 320-343, 2008.
831 Sutton, M. A., Tang, Y. S., Miners, B., and Fowler, D.: A New Diffusion Denuder
832 System for Long-Term, Regional Monitoring of Atmospheric Ammonia and
833 Ammonium, Water Air & Soil Pollution Focus, 1, 145-156, 2001.
834 Tørseth, K., Aas, W., Breivik, K., Fjæraa, A. M., Fiebig, M., Hjellbrekke, A. G., Lund
835 Myhre, C., Solberg, S., and Yttri, K. E.: Introduction to the European Monitoring and
836 Evaluation Programme (EMEP) and observed atmospheric composition change
837 during 1972–2009, Atmos. Chem. Phys., 12, 5447-5481,
838 10.5194/acp-12-5447-2012, 2012a.
839 Tørseth, K., Aas, W., Breivik, K., Fjæraa, A. M., Fiebig, M., Hjellbrekke, A. G., Lund
840 Myhre, C., Solberg, S., and Yttri, K. E.: Introduction to the European Monitoring and
841 Evaluation Programme (EMEP) and observed atmospheric composition change

during 1972-2009, Atmospheric Chemistry and Physics, 12, 5447-5481, 2012b.

Tevlin, A. G., Li, Y., Collett, J. L., Mcduffie, E. E., Fischer, E. V., and Murphy, J. G.: Tall Tower Vertical Profiles and Diurnal Trends of Ammonia in the Colorado Front Range, Journal of Geophysical Research Atmospheres, 122, 2017.

Van, D. A., Martin, R. V., Spurr, R. J., and Burnett, R. T.: High-Resolution Satellite-Derived PM2.5 from Optimal Estimation and Geographically Weighted Regression over North America, Environmental Science & Technology, 49, 10482-10491, 2015.

Van, D. A., Martin, R. V., Brauer, M., Hsu, N. C., Kahn, R. A., Levy, R. C., Lyapustin, A., Sayer, A. M., and Winker, D. M.: Global Estimates of Fine Particulate Matter using a Combined Geophysical-Statistical Method with Information from Satellites, Models, and Monitors, Environmental Science & Technology, 50, 3762, 2016.

Van Damme, M., Clarisse, L., Dammers, E., Liu, X., Nowak, J., Clerbaux, C., Flechard, C., Galy-Lacaux, C., Xu, W., and Neuman, J.: Towards validation of ammonia (NH_3) measurements from the IASI satellite, Atmospheric Measurement Techniques, 7, 12125-12172, 2014a.

Van Damme, M., Clarisse, L., Heald, C., Hurtmans, D., Ngadi, Y., Clerbaux, C., Dolman, A., Erisman, J. W., and Coheur, P.-F.: Global distributions, time series and error characterization of atmospheric ammonia (NH_3) from IASI satellite observations, Atmospheric Chemistry and Physics, 14, 2905-2922, 2014b.

Van Damme, M., Wichink Kruit, R., Schaap, M., Clarisse, L., Clerbaux, C., Coheur, P. F., Dammers, E., Dolman, A., and Erisman, J.: Evaluating 4 years of atmospheric ammonia (NH_3) over Europe using IASI satellite observations and LOTOS-EUROS model results, Journal of Geophysical Research: Atmospheres, 119, 9549-9566, 2014c.

Van Damme, M., Erisman, J. W., Clarisse, L., Dammers, E., Whitburn, S., Clerbaux, C., Dolman, A. J., and Coheur, P. F.: Worldwide spatiotemporal atmospheric ammonia (NH_3) columns variability revealed by satellite, Geophysical Research Letters, 42, 8660-8668, 2015.

Van Damme, M., Whitburn, S., Clarisse, L., Clerbaux, C., Hurtmans, D., and Coheur,

P. F.: Version2 of the IASI NH_3 neural network retrieval algorithm: near-real-time and reanalysed datasets, Atmospheric Measurement Techniques, 10, 1-14, 2017.

Van Damme, M., Clarisse, L., Whitburn, S., Hadji-Lazaro, J., Hurtmans, D., Clerbaux, C., and Coheur, P.-F.: Industrial and agricultural ammonia point sources exposed, Nature, 564, 99-103, 10.1038/s41586-018-0747-1, 2018.

Wang, Q., Jacob, D. J., Fisher, J. A., and Mao, J.: Sources of carbonaceous aerosols and deposited black carbon in the Arctic in winter-spring: implications for radiative forcing, Atmospheric Chemistry and Physics Discussions, 11, 19395-19442, 2011.

Wang, Y., Logan, J. A., and Jacob, D. J.: Global simulation of tropospheric O 3 -NO x -hydrocarbon chemistry: 2. Model evaluation and global ozone budget, Journal of Geophysical Research Atmospheres, 103, 10727-10755, 1998.

Warner, J. X., Wei, Z., Strow, L. L., Dickerson, R. R., and Nowak, J. B.: The global tropospheric ammonia distribution as seen in the 13-year AIRS measurement record, Atmospheric Chemistry and Physics, 16, 5467-5479, 2016.

Warner, J. X., Dickerson, R. R., Wei, Z., Strow, L. L., Wang, Y., and Liang, Q.: Increased atmospheric ammonia over the world's major agricultural areas detected from space, Geophysical Research Letters, 10.1002/2016GL072305, 2017.

Wesely, M.: Parameterization of surface resistances to gaseous dry deposition in regional-scale numerical models, Atmospheric Environment, 23, 1293-1304, 1989.

Whitburn, S., Van Damme, M., Kaiser, J. W., van der Werf, G. R., Turquety, S., Hurtmans, D., Clarisse, L., Clerbaux, C., and Coheur, P. F.: Ammonia emissions in tropical biomass burning regions: Comparison between satellite-derived emissions and bottom-up fire inventories, Atmospheric Environment, 121, 42-54, https://doi.org/10.1016/j.atmosenv.2015.03.015, 2015.

Whitburn, S., Van Damme, M., Clarisse, L., Bauduin, S., Heald, C. L., Hadji-Lazaro, J., Hurtmans, D., Zondlo, M. A., Clerbaux, C., and Coheur, P. F.: A flexible and robust neural network IASI-NH_3 retrieval algorithm, Journal of Geophysical Research: Atmospheres, 121, 6581-6599, 10.1002/2016JD024828, 2016.

Xia, Y., Zhao, Y., and Nielsen, C. P.: Benefits of China's efforts in gaseous pollutant control indicated by the bottom-up emissions and satellite observations 2000–2014,

902 Atmospheric Environment, 136, 43-53,
903 http://dx.doi.org/10.1016/j.atmosenv.2016.04.013, 2016.
904 Xu, W., Luo, X. S., Pan, Y. P., Zhang, L., Tang, A. H., Shen, J. L., Zhang, Y., Li, K. H.,
905 Wu, Q. H., Yang, D. W., Zhang, Y. Y., Xue, J., Li, W. Q., Li, Q. Q., Tang, L., Lv, S. H.,
906 Liang, T., Tong, Y. A., Liu, P., Zhang, Q., Xiong, Z. Q., Shi, X. J., Wu, L. H., Shi, W.
907 Q., Tian, K., Zhong, X. H., Shi, K., Tang, Q. Y., Zhang, L. J., Huang, J. L., He, C. E.,
908 Kuang, F. H., Zhu, B., Liu, H., Jin, X., Xin, Y. J., SHi, X. K., Du, E. Z., Dore, A. J.,
909 Tang, S., Collett Jr, J. L., Goulding, K., Sun, Y. X., Ren, J., Zhang, F. S., and Liu, X. J.:
910 Quantifying atmospheric nitrogen deposition through a nationwide monitoring
911 network across China, Atmospheric Chemistry and Physics, 15, 12345-12360, 2015.
912 Xu, W., Song, W., Zhang, Y., Liu, X., Zhang, L., Zhao, Y., Liu, D., Tang, A., Yang, D.,
913 and Wang, D.: Air quality improvement in a megacity: implications from 2015 Beijing
914 Parade Blue pollution control actions, Atmospheric Chemistry and Physics, 17, 31-46,
915 2017.
916 Yu, Y., Xu, M., Yao, H., Yu, D., Qiao, Y., Sui, J., Liu, X., and Cao, Q.: Char
917 characteristics and particulate matter formation during Chinese bituminous coal
918 combustion, Proceedings of the Combustion Institute, 31, 1947-1954,
919 http://dx.doi.org/10.1016/j.proci.2006.07.116, 2007.
920 Zhang, L., Gong, S., Padro, J., and Barrie, L.: A size-segregated particle dry
921 deposition scheme for an atmospheric aerosol module, Atmospheric Environment, 35,
922 549-560, http://dx.doi.org/10.1016/S1352-2310(00)00326-5, 2001.
923 Zhang, L., Chen, Y., Zhao, Y., Henze, D. K., Zhu, L., Song, Y., Paulot, F., Liu, X., Pan,
924 Y., and Huang, B.: Agricultural ammonia emissions in China: reconciling bottom-up
925 and top-down estimates, Atmospheric Chemistry & Physics, 18, 1-36, 2017a.
926 Zhang, X., Wu, Y., Liu, X., Reis, S., Jin, J., Dragosits, U., Van Damme, M., Clarisse,
927 L., Whitburn, S., Coheur, P.-F., and Gu, B.: Ammonia Emissions May Be
928 Substantially Underestimated in China, Environmental Science & Technology, 51,
929 12089-12096, 10.1021/acs.est.7b02171, 2017b.
930 Zhang, Y., Mathur, R., Bash, J. O., Hogrefe, C., Xing, J., and Roselle, S. J.: Long-term
931 trends in total inorganic nitrogen and sulfur deposition in the U.S. from 1990 to 2010,

932 Atmospheric Chemistry & Physics, 1-27, 2018.
933 Zhu, L., Henze, D. K., Cady-Pereira, K. E., Shephard, M. W., Luo, M., Pinder, R. W.,
934 Bash, J. O., and Jeong, G. R.: Constraining U.S. ammonia emissions using TES
935 remote sensing observations and the GEOS‐Chem adjoint model, Journal of
936 Geophysical Research Atmospheres, 118, 3355-3368, 2013.
937
938

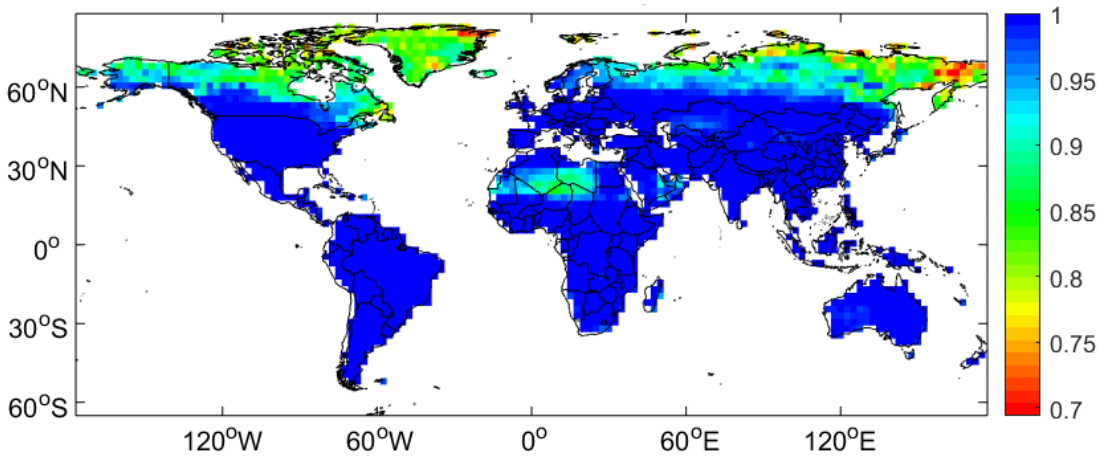

Fig. 1 R^2 of Gaussian fit for NH_3 vertical profiles.

943

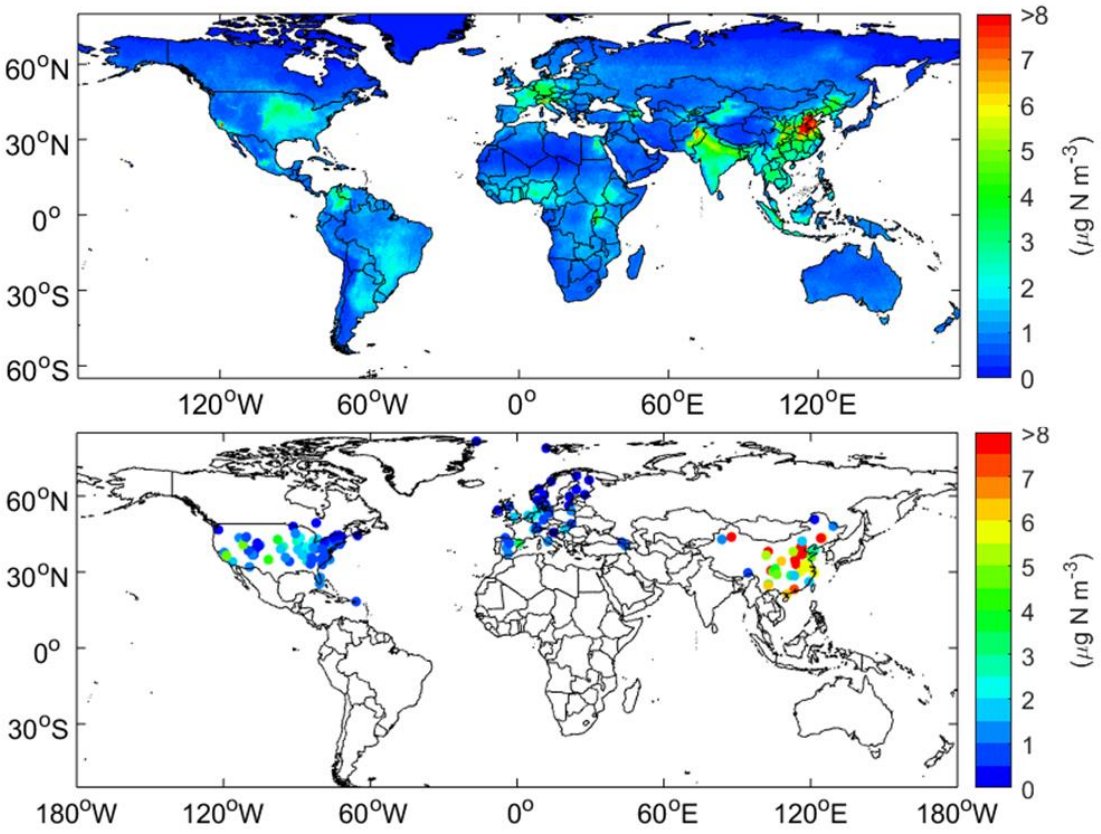

944

945 **Fig. 2** Spatial distribution of satellite-derived and measured surface NH_3 concentrations in 2014.

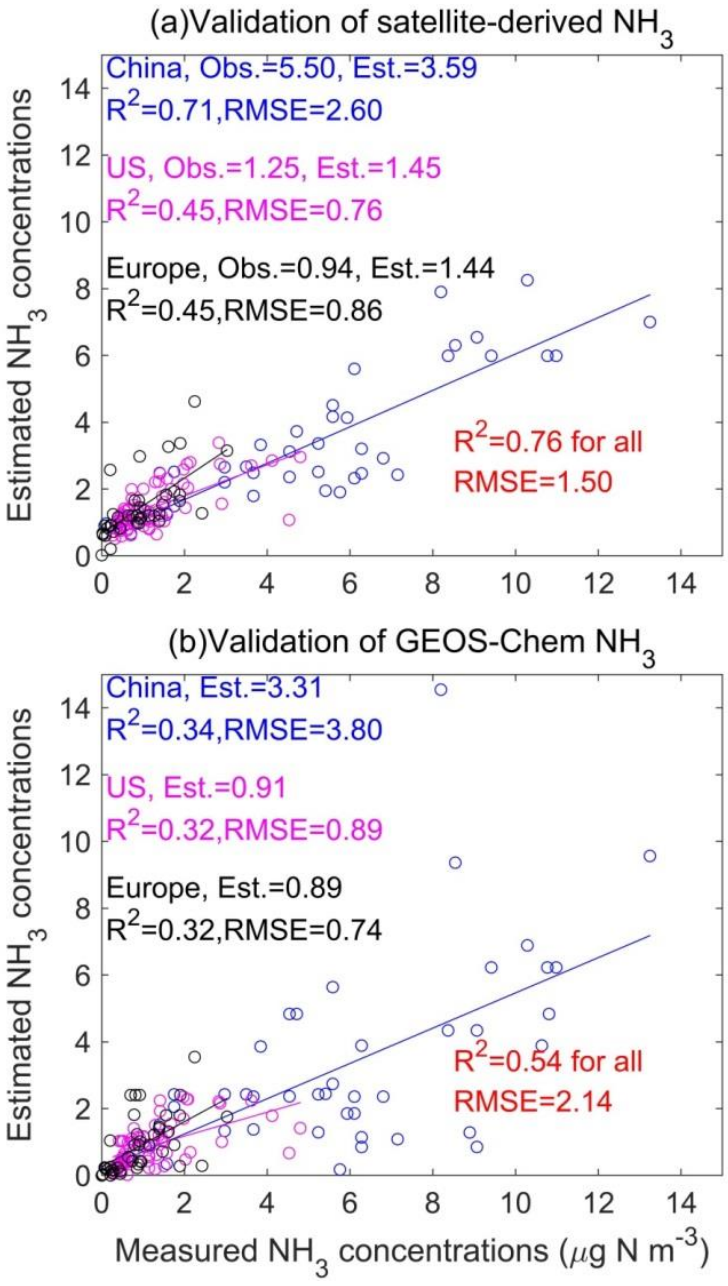

946

947 **Fig. 3** Comparison of satellite-derived and GEOS-Chem modelled surface NH_3 concentrations with
948 measured concentrations in China, US and Europe.

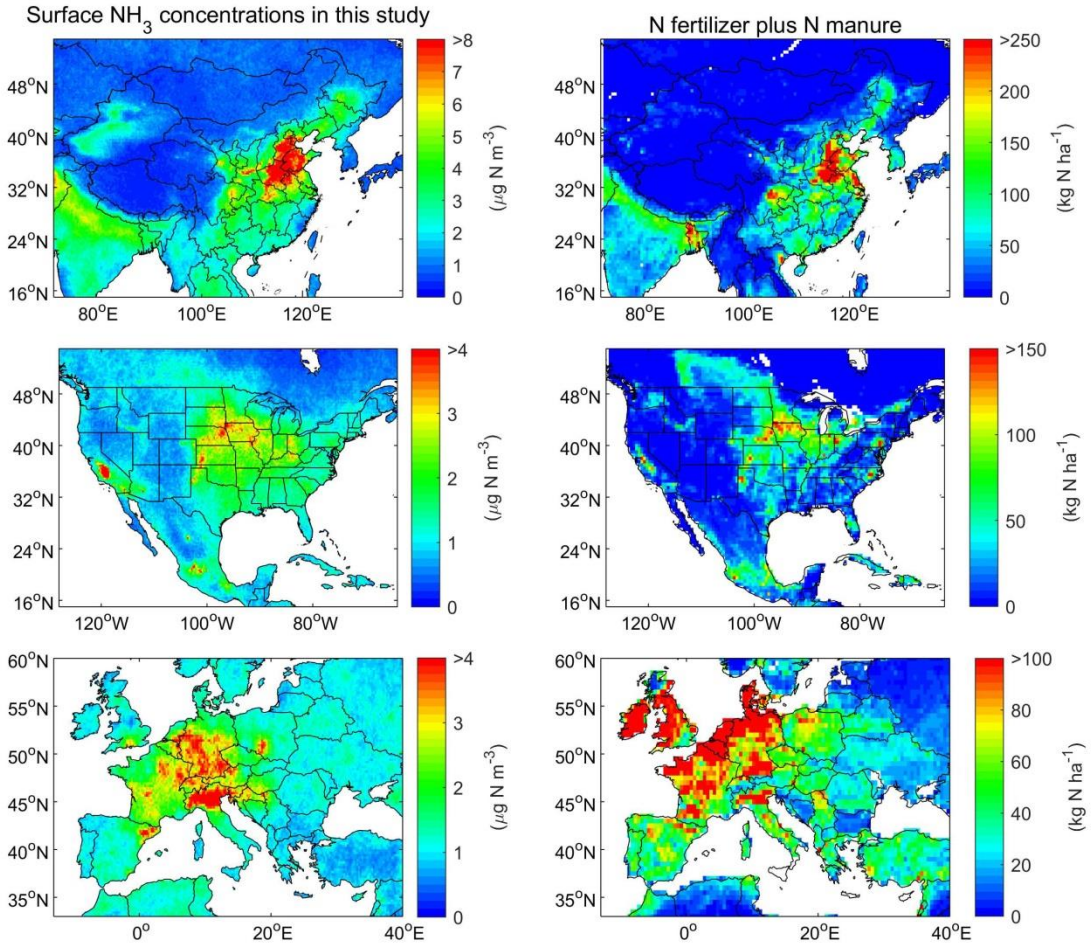

949

950 **Fig. 4** Spatial distribution of IASI-derived surface NH_3 concentrations, and N fertilizer plus N manure
951 in China, Europe and US.

952

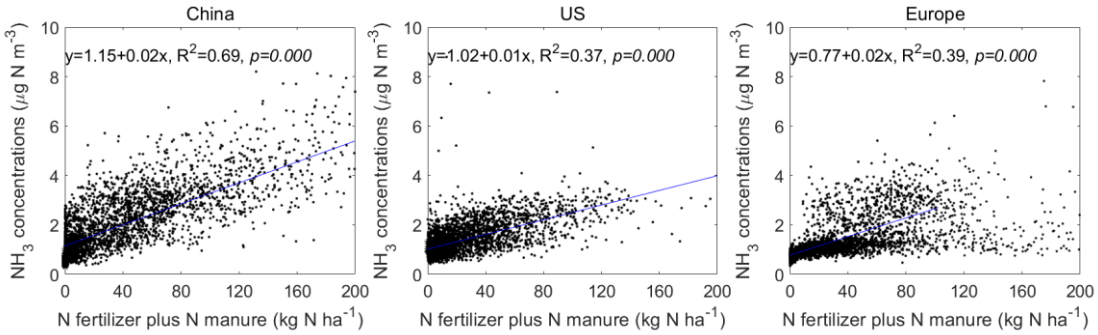

Fig. 5 Comparison of satellite-derived surface NH_3 concentrations and N fertilizer plus N manure in China, US and Europe. The spatial resolution of satellite-derived surface NH_3 concentrations and N fertilizer plus N manure is 0.25° and 0.5°, respectively. We firstly resampled the satellite-derived surface NH_3 concentrations to 0.5° grids, and then compared it with N fertilizer plus N manure by each grid cell. We obtained the N fertilizer and N manure data produced from McGill University (Potter et al., 2010).

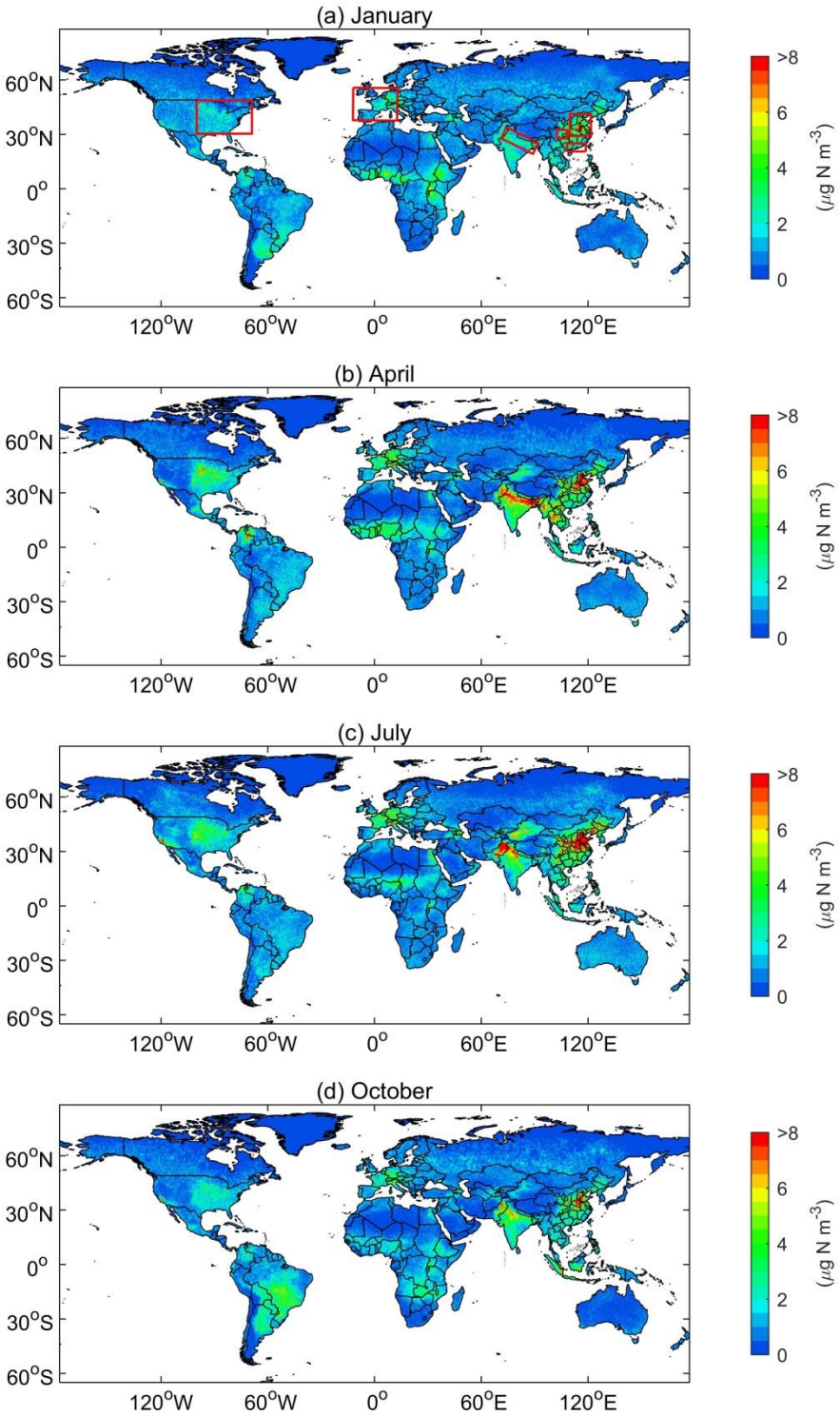

Fig. 6 Global surface NH_3 concentrations in January, April, July and October in 2014. The red rectangular regions include East China (ECH), Sichuan and Chongqing (SCH), Guangdong (GD), Northeast India (NEI), East US (EUS) and West Europe (WEU).

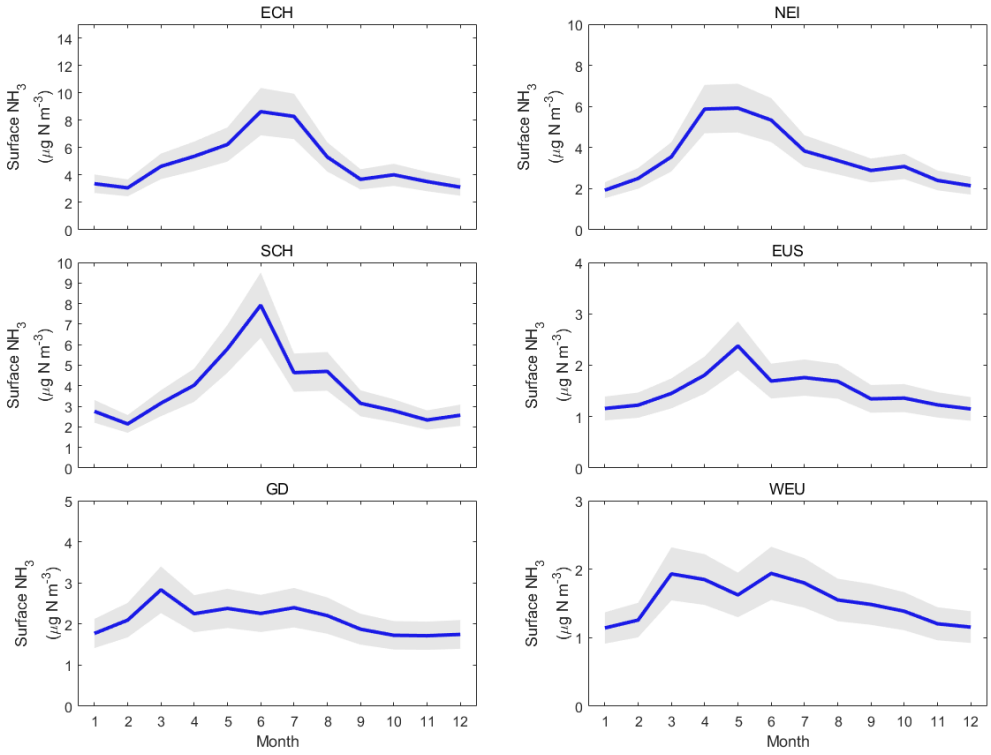

Fig. 7 Monthly variations of surface NH_3 concentrations in hotspot regions including East China (ECH), Sichuan and Chongqing (SCH), Guangdong (GD), Northeast India (NEI), East US (EUS) and West Europe (WEU).

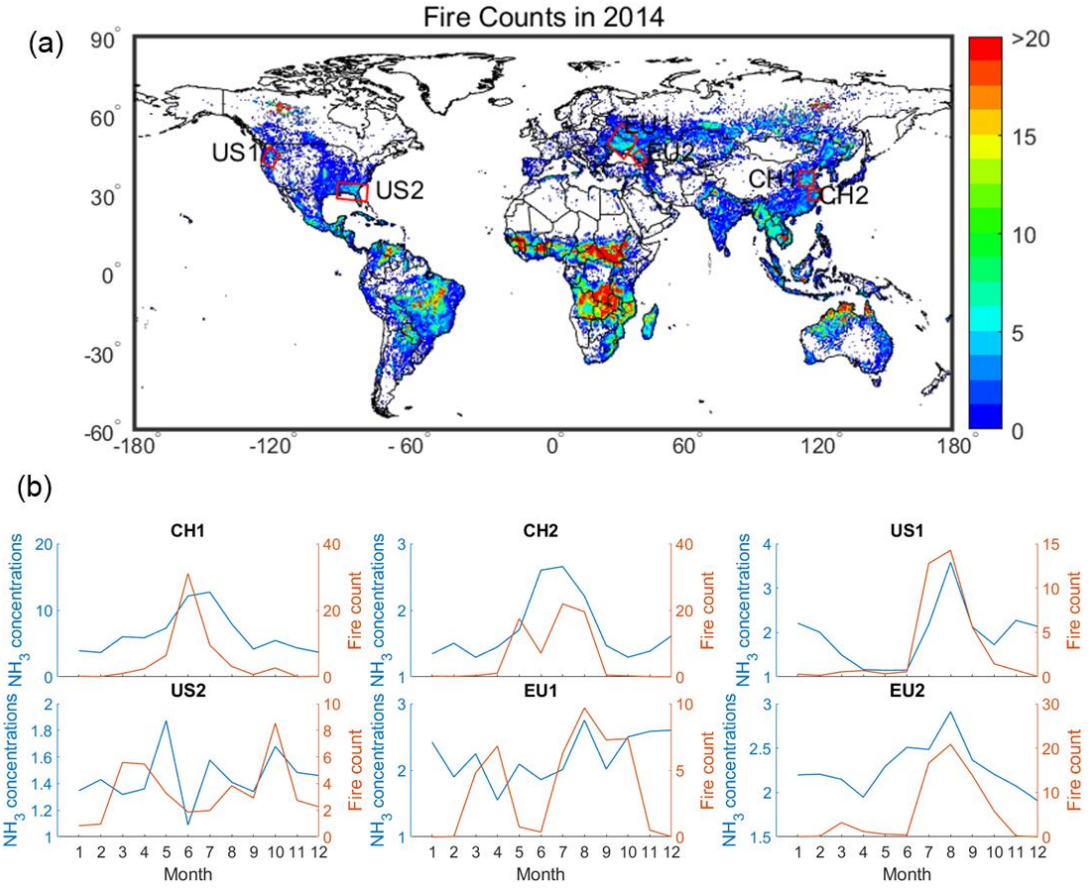

Fig. 8. Total raw fire count from the MODIS in 2014 (a), and monthly variations of fire counts and surface NH_3 concentrations in biomass burning regions in China, the US and Europe (b).

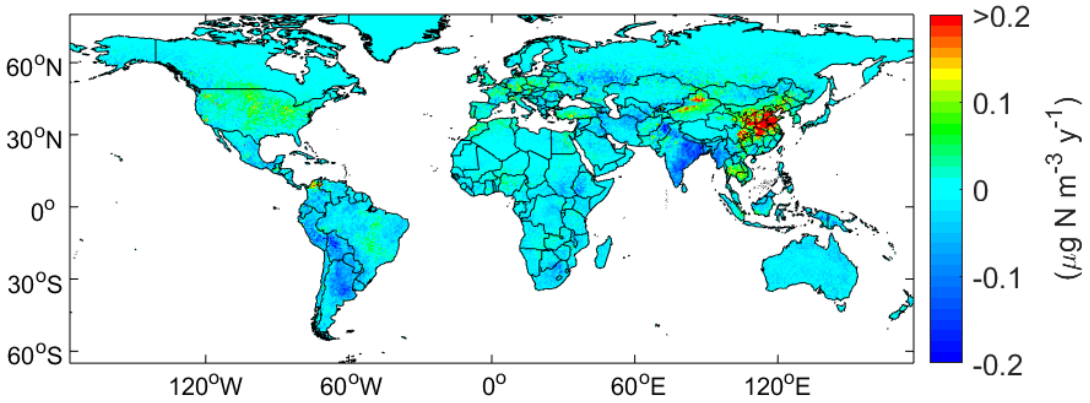

Fig. 9 Trends of IASI-derived surface NH_3 concentrations between 2008 and 2016. A linear regresion was perfomed to calculate the trends. The significance value (p) and R^2 for the trends can be found in **Fig. S10**.